Sci. Rep. RITU A44 (1997) pp. 113-143
No. 2, March 1997

Scanning Tunneling Microscopy of the GaAs(001) Surface Reconstructions *

Qi Kun Xue, [a] Tomihiro Hashizume, [b] Ayahiko Ichimiya, [c] Takahisa Ohno, [d] Yukio Hasegawa[a] and Toshio Sakurai[a]

[a] *Institute for Materials Research (IMR), Tohoku University, Sendai 980, Japan*
[b] *Advanced Research Laboratory, Hitachi Lid., Saitama 350-03, Japan.*
[c] *Applied Physics Department, Nagoya University, Nagoya, Japan.*
[d] *National Research Institute for Metals, Tsukuba, Ibaragi 305, Japan.*

(Received January 25, 1997)

The atomic structure of the GaAs(001) surface has been disputed since molecular beam epitaxy (MBE) technique was developed in the earlier nineteen sixties. The invention of scanning tunneling microscopy (STM) with its real-space atom-resolution capability, has revolutionized the situation. This paper reviews the STM investigations of the principal reconstructions found on the GaAs(001) surface, As-rich 2x4 and 2x6, Ga-rich 4x2 and 4x6. These studies, together with advanced theoretical analyses, have finally resulted in establishment of a unified structural model for various reconstructions, with which we can explain most of the observations and long-standing controversies about the atomic structures and surface stoichiometries.

KEYWORDS: GaAs, scanning tunneling microscopy, molecular beam epitaxy, reflection high energy electron diffraction, first-principles total energy calculation.

1. Introduction

Because of its zinc blend crystal structure with a tetrahedral coordination in the bulk, the polar GaAs(001) surface could be terminated with either As or Ga atoms. Depending on the surface coverage and the experimental conditions of molecular beam epitaxy (MBE), the (001) surface exhibits a number of reconstructions, starting with the most As-rich phase which has a c(4x4) symmetry, through the 2x4 (including the off-phase c(2x8)), 2x6, 4x6, ending with the 4x2 (including the off-phase c(8x2)) Ga-stabilized phase [1-13]. In addition, there have been several transient or adsorbate-induced structures such as 2x3, 2x1, c(6x4), 3x1 and 3x6 etc. reported, implying the rather complicated nature of the GaAs(001) surface.

It is well-known that the MBE growth of GaAs(001) is usually performed under the conditions which lead to an As-terminated 2x4 reflection high energy electron diffraction (RHEED) pattern. As the most common and important structure in the technological applications of MBE, the 2x4 reconstruction including the more As-rich c(4x4) has been most extensively studied in the past by means of almost all surface sensitive techniques. These include RHEED [6,10,11,14-22,28], low-energy electron diffraction /Auger electron spectroscopy (LEED/AES) [7,8,23,24], photoemission spectroscopy (PES) [12,25,26], work function measurement [24], X-ray diffraction [27], X-ray photoelectron diffraction (XPD) [28], reflectance-difference spectroscopy (RDS) [29], high resolution electron energy loss spectroscopy (HREELS) [13], secondary electron intensity measurement [30], medium-energy ion scattering (MEIS) [31] and scanning tunneling microscopy (STM) [32-52]. Total energy electronic structure calculations have also been employed lately to examine the energetics in determining the geometric and electronic structures of the surface [53-58]. These studies have rendered a general yet clear picture on atomic details of the 2x4 surface.

On the other hand, relatively little attention has been directed toward the surface reconstructions in the Ga-rich regime, such as 4x2, 2x6 and 4x6 [3]. This simply arises from the fact that the preparation of Ga-rich surfaces, and thus their detailed study, are significantly more difficult. Especially, the preparation of as-deposited Ga-rich surfaces is nearly impossible under the extremely As-rich atmosphere (10^{-6} - 10^{-4} Torr), where the standard MBE growth of GaAs is being carried out. Almost all previous works for the Ga-rich phases began with the As-capped surface, and it was attempted to prepare the Ga-rich phases by trial-and-error annealing procedures, which are known to be unreliable in producing high quality ordered surfaces. Indeed, there is a very narrow surface composition range for the 4x2 surface, and thus, it is an insurmountable task to obtain it by this post-growth annealing [9]. Neverthless, in order to achieve a comprehensive understanding of the growth kinetics and mechanisms of the bi-layer MBE growth on the GaAs(001), a complete knowledge of both As-rich and Ga-rich surfaces is needed, since the growing front must be terminated with the alternative 2x4-As and 4x2 or other Ga-rich surface [14,17].

Earlier investigations have shown a close relationship between the surface reconstruction and the surface stoichiometry, but a clear picture on their relationship has not been obtained until now. Many efforts have been rendered, since the earliest stage of the MBE technique

*IMR, Report No. 2085

development, to quantify surface stoichiometry and its relationship with phase structure by many groups using various technique. These investigations provided valuable information on the surface stoichiometry for almost all the known GaAs(001) reconstructions. However, for each surface phase being studied, there are considerable discrepancies among the reported values [7-9,12,20,61]. Unlike its elemental counterparts (such as Si, Ge), the GaAs has an additional composition degree of freedom, and both of the elements may be involved in the reconstruction process. It was also reported that, for some given reconstruction (e.g., the 4x6 discussed in this paper), there may be a wide composition range for which two or more structures may co-exist [20]. Depending on the thermodynamic and kinetic aspects of the surface preparation procedure, the structures associated with different As(Ga) concentration ratios may appear in the surface with changing domain sizes.

This type of local configuration cannot be sorted out easily by these semi-macroscopic conventional techniques, since the surface inhomogeneity both parallel and perpendicular to the surface is averaged over the probing area. Therefore, it is rather difficult to determine the surface composition without detailed knowledge of the structure of the surface. On the other hand, most of the structural determination on the surface reconstructions has been performed mainly by diffraction techniques. These techniques are useful for surveying surface symmetry, but yield only long-range ordering information of the surface (in the reciprocal space). Realizing the comparatively large and complex unit cell of the GaAs(001) surface and involvement of the two different species at the surface layers, an unambiguous interpretation of the diffraction data is a great challenge.

1.1. Electron counting model [59]

Based on these experimental and theoretical studies, two basic and general features on the structure of the GaAs(001) surface have emerged. As seen below, these two features and the stability of all reconstructions of the GaAs(001), including many other low-index compound semiconductor surfaces, can be substantiated by a simple rule–the so-called electron counting model (ECM) [59], now let's first discuss this rule.

The atoms in bulk GaAs are sp^3 hybridized. Two hybridized orbitals, one from each type of atom. combine to form a bonding and antibonding orbital. At the surface, some hybrid orbitals cannot form bonds, therefore, if no reconstruction occurs, partially filled sp^3 dangling bonds will remian. In reality, this configuration is unstable, thus in order to reduce the number of dangling bonds and decrease the surface energy, the adjacent As (Ga) atoms form a dimer along the [$\bar{1}$10] ([110]) direction and reconstruct with 2x (x2) periodicity, similar to the case of the Si(001) surface [3]. This characterizes the first feature of the GaAs(001) surfaces: dimerization. The second is due to the different dangling bond levels of the surface As and Ga. The energy levels of these dangling bonds can be estimated from the energies of the s and p atomic levels from which they are derived [60]. Based on Harrison's estimation, as shown in Fig.1, the dangling-bond energy level (E_h(As)) of As lies below the valence-band maximum of the bulk semiconductor and should be filled, whereas the dangling-bond energy level (E_h(Ga)) of Ga lies above the bulk conduction-band minimum and should be empty. In order to achieve this, electrons transfer from the dangling bonds of the electropositive element (As) to the dangling bonds of the electronegative element (Ga). However, the charge transfer induces a rather larger static-electric capacitance energy due to charge accumulation, the resulting surface becomes energitically unstable unless some amount of the dimers is removed from the surface, i.e., dimer missing, the second feature of the reconstructions on the GaAs(001). The scheme was generalized as the ECM by Pashley [60], which requires that, a stable surface structure is found where the number of available electrons in the surface layer will exactly fill all dangling bond states in the valence band, leaving those in the conduction band empty. This condition will necessarily result in there being no net surface charge, then the surface will be semiconducting, whereas partially filled dangling bonds may lead to a metallic surface.

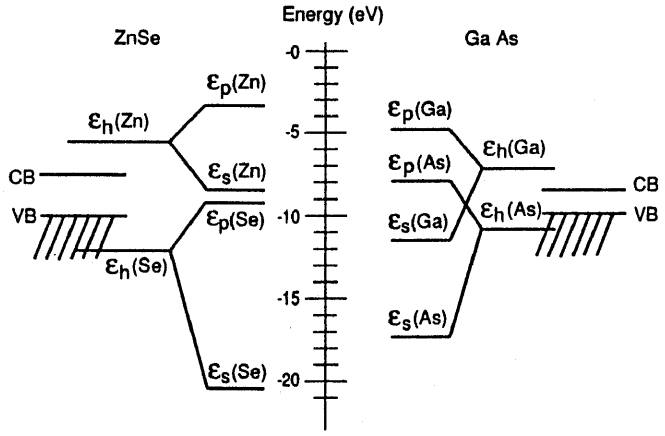

Figure 1. The energy levels E_h of the sp^3 dangling bond states of GaAs. The energies are derived from the energies of the s and p orbitals, E_s and E_p, respectively. The data are from Harrison[60]

1.2. The 2x4/c(2x8) reconstruction

Instead of assuming asymmetric As dimers for explaining the 4x periodicity along the [110] direction [12,25], the idea of "As dimer vacancy" was introduced theoretically to explain the 2x4 reconstruction by Chadi[53] and was first confirmed experimentally by using STM [32]. According to ECM, the simplest structure for the 2x4 unit structure to conserve the charge neutrality can be achieved by removing one As dimer from every four As dimers [60].

Although it is now well established and accepted that the (2x4) symmetry is constructed from As dimers and As dimer vacancies, there are some controversial models of the (2x4) unit structures suggesting the presence of Ga on the top layer [31]. Based on tight-binding total-energy calculations, Chadi proposed two possible mod-

els, (a) three As dimers and one dimer vacancy in a unit (Fig. 2(a)) and (b) two As dimers and two dimer vacancies in a unit (Fig. 2(b)) at the outermost surface layer [53]. In the case of model (b), one of the second layer Ga pairs is also removed. Although both models are calculated to have almost the same stability in energy, the model (b), two As-dimer model, was discarded later by Larsen and Chadi based on the growth kinetics consideration [16]. Chadi also pointed out another possible vacancy model which retains all of the four pairs of the second layer Ga atoms (Fig. 2(c)) [53]. However, the total energy of this model is higher by 1.6eV per unit than models (a) and (b) and was discarded [53].

Undisputable confirmation of the As vacancy model was given by the first STM observation by Pashley et al. [32]. They prepared the sample in an *ex-situ* MBE system, capped the sample with As for protection prior to transferring the sample through air into the STM apparatus and removed the As overlayers by a brief heating before the STM study. The STM images clearly showed that the (2x4) periodicity is due to a regular array of As dimers and As dimer vacancies. They also discussed on an antiphase boundary along the [$\bar{1}$10] direction which produces the c(2x8) phase from the (2x4) unit. By analyzing their images of the (2x4) unit, they concluded that the STM images are accounted best by the three As-dimer model by Chadi (Fig. 2(a)). Biegelsen et al. prepared the sample in the in-situ MBE chamber and reported that the (2x4) phase consisted of three As dimers at the outermost surface layer [33], supporting the Pashley's observation [32]. However, they also observed the (2x4) unit consisting of two As dimers at the outermost surface layer when the surfaces was annealed longer or at higher temperatures or grown with lower As_4/Ga flux ratios [33].

The situation is complicated by the behavior of the 2x4 reconstruction as a function of the growth conditions. Three different phases (the α, β, and γ phases) of the surface have been identified by RHEED experiments, depending on the characteristics in the fractional order (1/4th, 2/4ths and 3/4ths) RHEED spot intensities and preparation conditions [17]. The α phase occurs at the highest substrate temperatures with relatively weak 2/4ths spot intensity compared with 1/4th and 3/4ths intensities, the γ phase is formed in the lowest substrate temperature range and its 2/4ths spot is almost absent. The β phase exists between these two and the 2/4ths spot is strong and equal to 1/4th and 3/4ths. They performed a kinematical RHEED calculations to analyze these data and proposed that the outermost unit structure of the α, β, and γ phases as follows (PF scheme). The α phase is made of two As dimers (Fig. 2(d); with the second layer Ga dimerization). This model assigned for the α phase was later examined by Northrup and Froyen (NF) [56] and the relaxation of the second layer Ga atoms was introduced for the stability of the model (Fig. 2(e)). The unit structure of the β phase PF proposed is the Chadi's three As dimers (Fig. 2(a)). And the γ phase is assigned to the model which has an extra As dimer sitting on the β surface along the [110] direction (Fig. 2(f)) [17]. Based on the FP scheme, the As coverage is 0.5ML for α phase, 0.75ML for the β phase and 1.0ML for the γ phase, consistent with that expected from the preparation condition for each phase.

Many people have been using the FP scheme since then: three or two As-dimer model was chosen depending on the experimental conditions and obtained results. The important problem for the GaAs(001) 2x4 phases appeared to be solved [19-22,2829,55,56]. However, Heller et al. recently reported based on their in-situ STM observations that the two As-dimer unit at the outermost surface layer is dominant and claimed that the three As-dimer unit exists only under special circumstances [35], and the two As-dimer unit is always dominant in most STM experiments later on [36, 38,39,44,46-48,50,51], even in the case of fluid conditions [45]. In contrast, Gallagher et al. [37] and Broekman et al. [49] analyzed their STM images and supported the three As-dimer unit. Recently, Falta et al. performed a MEIS experiment on the ex-situ (decapped) MBE-grown GaAs(001) surfaces and proposed a radically new model that the first layer of the (2x4) phase may contain both Ga and As atoms, in contrast to the commonly accepted As terminated models [31].

1.3. The Ga-rich 4x2 and 4x6 Reconstructions

Since the pioneering MBE-RHEED work by Cho [2, 3], now it is well accepted for the 4x2 reconstruction that the two-fold (2x) periodicity is due to bond-pairing of the surface Ga dangling bonds along the [110] direction and the four-fold (x4) periodicity comes from regular Ga-dimer missing, same to the situation on the As-rich 2x4 surface, but now the surface dimers rotate 90° along the (001) crystal axis. Based on their HREELS data, Frankel et al. [13] proposed the first structural model for the 4x2 surface, concluding that the four-fold (4x) periodicity is due to the formation of three Ga-dimers and one missing Ga-dimer for a unit cell, as shown in Fig. 3(a). This three-dimer model contains 3/4 of a monolayer (ML) of the Ga-dimers on top of a full monolayer As-terminated surface. If the groups of three Ga dimers are arranged in phase with the adjacent groups in the bonding direction, the resulting structure is 4x2, while the out-of-phase arrangement gives rise to the c(8x2) translational symmetry, which is consistent with existing LEED, AES, RHEED and UPS results [6-8].

The absence of some of the surface dimers has been directly confirmed by two previous STM investigations [33,61]. Both observations revealed only two Ga dimers in a unit cell. Shown in Fig.3(b) is the atomic model (referred to as Ga-bilayer model hereafter) proposed by Biegelsen et al.[33] on the basis of the first STM observation of this surface. In order to maintain the charge neutrality [14,17,59], the two-fold coordinated As atoms in the second layer exposed by two-dimer vacancy are removed, and the third layer Ga atoms are dimerized and three-fold coordinated.

The atomic model proposed by Skala et al. (referred

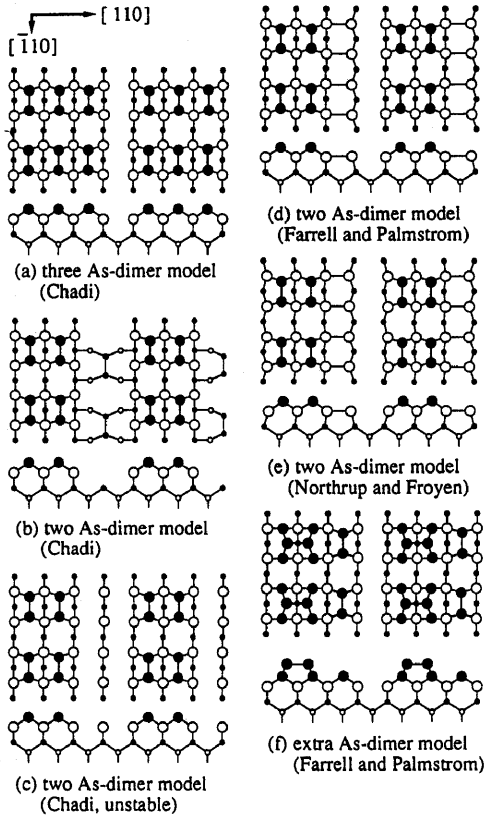

Figure 2. Schematic representations of the GaAs(001)-(2x4) surface reconstruction models. (a) three As-dimer by Chadi[53] and (b) two As-dimer models proposed by Chadi[61] (c) (unstable) two As-dimer model by Chadi[53] (d) two As-dimer model proposed by FP for the (2x4)-α phase[14,17] (e)model (d) modified including the second-layer Ga relaxation by NF[56] and (f) extra As-dimer model proposed by FP for the (2x4)-γ phase[14,17] Filled circles denote As atoms and open circles denote Ga atoms. Both top and side views are shown for each model. The As surface coverages are (a) 0.75ML, (b) 0.75ML, (c) 0.5ML, (d) 0.5ML, (e) 0.5ML and (f) 1ML.

to as As-model hereafter) [61] consists of two As dimers in the first layer and two Ga dimers in the second layer in a unit cell (shown in Fig.3(c)). They claim, surprisingly, that the outermost surface layer is As, not Ga, which is radically different from other Ga-rich models. We surmise that the main reason for such a radically different identification over the Ga-model is the experimental finding that the faint features assigned to the Ga-dimers in the STM image are positioned in between the bright individual humps which are identified as As along the [$\bar{1}$10] direction which cannot be explained readily by the Ga-bilayer model.

If one adopts the general rules that the 4x2 surface is terminated with Ga dimer as speculated by Frankel et al. [13] and Biegelsen et al. [33] and that the necessary charge transfer takes place according to ECM employed to examine semiconductor surface reconstruction [59], this surface is quite unique and puzzling in interpreting STM images. *The filled dangling bond orbitals of the Ga dimer locating in the first layer has relatively low local density of states (LDOS) which possesses a large energy dispersion from -1.9 to -0.5 eV [62]. The occupied As dangling bond orbitals have predominantly high LDOS, but the As atoms are geometrically placed in the second layer, lower than the first layer Ga by as much as 1.4Å.* At the negative bias voltage of -2 eV, both of these Ga and As orbitals overlap to some extent and are accessible to the tunneling process, hence are imaged by STM. Since STM maps the local density of states of the surface, not simply the atomic geometry of the surface, the correct interpretation of the STM image requires the knowledge of surface charge density distribution unique to the models. Therefore, the discrepancies in the Ga- and As- models mentioned above cannot be resolved by these two STM investigations alone. The electron counting rules are also not likely to sort out the problem because the necessary charge neutrality condition was already taken account into when the authors proposed the models.

Similar to what they speculated for the As-rich 2x4, Falta et al. proposed the mixed Ga/As model, based on their MEIS experiment and its Monte Carlo simulations [31]. According to them, the configuration of the atoms in the reconstructed surface layers is exactly the same as that of the Chadi's three As-dimer model for the 2x4 reconstruction [53], except it is rotated by 90°with respect to the (001) axis. However, they claimed that an interlayer Ga/As mixing must be considered for this surface. In order to explain the measured high Ga peak, certain amounts of replacement of the surface As atoms by the Ga in the second layer would be needed. They further suggested that this type of substitution or mixing phenomenon is not limited to the case of the 4x2 phase and is indeed universal for all other reconstructed surfaces of the GaAs(001). This mixed Ga/As model has, however, been disputed by several groups [63]. The surface coverage also varies from 0.5ML-As for As-model, 0.75ML-Ga for Ga-bilayer model (0.25 ML from the third layer Ga), 0.75ML-Ga for three Ga-dimer model, ~1ML for the mixed Ga/As model.

To clarify these experimental uncertainties and establish a reliable model for this surface, Northrup and Froyen [56,57] and Ohno [55] have performed a series of total energy theoretical calculations. Both groups concluded that the substitution model by Falta et al. is not likely to occur in the entire As/Ga ratio composition. Although the As/Ga replacement still maintain the necessary charge neutrality, it significantly changes the bonding nature. The calculation shows that the minimum energy cost is 0.67 eV for each As-Ga replacement, therefore, this structure is not stable. Northrup and Froyen pointed out that in the permitted range of values of Ga chemical potential, the Ga-bilayer model is the most energetically favorable among various models. The result by Ohno is also similar and will be discussed in later section. We have also reported [41-43] that our

STM study combined with the RHEED intensity dynamical calculation for the 2x4 surface is consistent with the Northrup and Froyen's theory. However, experimental data are not available to test the theory in the case of the 4x2 phase.

Even lesser understanding lies in the case of the 4x6 phase. There has been not a single structural model being proposed so far, most likely due to its large and complicated unit cell situation. It has been believed that this surface is a mixture of 4x1 and 1x6 reconstructed domains [8]. All published diffraction patterns have shown no spots with non-integral coordinates in both the [110] and [$\bar{1}$10] directions which demonstrates that a "genuine 4x6" reconstruction may not exist. However, by UHV annealing at temperatures higher that those necessary to establish the 4x2/c(8x2) structure, Biegelsen et al. reported the observation by LEED and STM of the genuine 4x6 reconstruction [33]. Unfortunately noisy tunneling current precluded them to obtain a high resolution STM image in order to document the atomic structure. Creighton concluded [64], based on the TMGa adsorption experiment, that the 1x6 and 4x6 and c(8x2) actually have the same stoichiometry since they all display the same chemistry for TMGa adsorption. He speculated that all Ga-rich surface phases can be constructed under a scheme of superposition idea starting from the 4x2 three Ga-dimer model. It was thought that this may be true in terms of surface stoichiometry, since several groups also pointed out that there is indeed little difference in stoichiometry between the 4x2 and 4x6 phases [8, 20]. On the other hand, Bachrach et al. [10] reported that the 4x6 phase is actually more As-rich than the 4x2 phase, while most experimental data supported that the 4x6 phase is more Ga-rich [8, 12, 20] and that the big difference (about 0.2ML As) in stoichiometry between the 4x6 and 4x2 reconstructions cannot be explained by superposition of the three dimer 4x2 sub-unit. An attempt was made to establish a surface phase diagram using the vicinal surface, even though there is no reliable equilibrium surface phase diagram for the GaAs(001) [18]. The result showed that two or more structures may usually overlaps on the Ga-rich regime [24].

We have overcome the difficulties in the preparation of high quality as-grown various GaAs(001) Ga-rich surfaces (c(4x4), 2x4, 2x6, 4x2 and 4x6) by introducing migration enhanced epitaxy (MEE) technique [41-43]. We were able to steadily follow the phase evolution among various phases by simply choosing appropriate As/Ga ratios and shutter operation pulse in MEE. Thus, we obtained atomically resolved STM images of the 2x4, 4x2, 4x6 and 2x6 phases. Combined with the advanced theoretical calculation by Ohno [55] and RHEED dynamical intensity analysis in collaboration with Ichimiya [65], we have overcome the difficulties in interpreting our high-resolution STM data in order to propose a unified structural model for the 2x4, 4x2 and 4x6 surfaces [43, 66]. We will show in the following sections that our model can explain most published results and resolve main controversies in the structures and compositions of various surface phases.

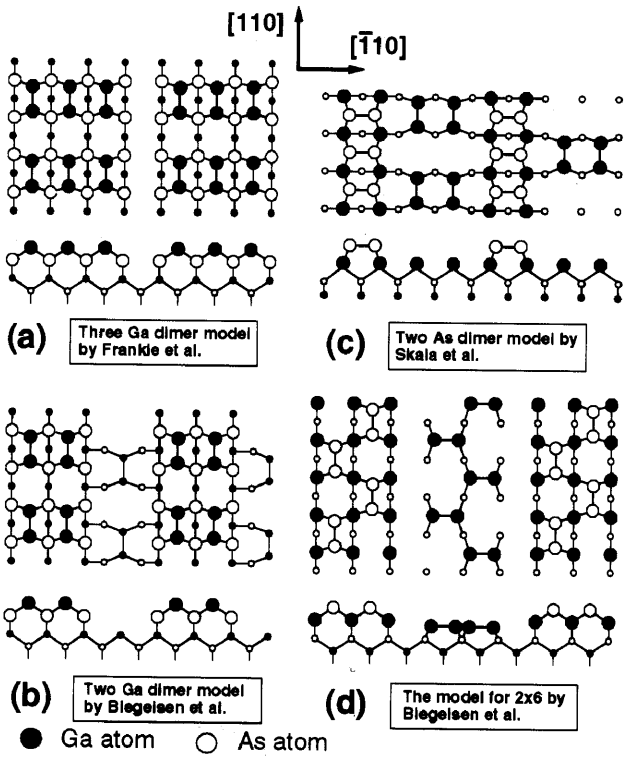

Figure 3. The ball-and-stick models for the 4x2 (a, b and c) and 2x6 (d) reconstructions. (a): three Ga-dimer model by Frankle et al.[13]. If some of the As atoms in the second layer are replaced with Ga atoms, it will lead to the mixed As/Ga model by Falta et al. [31]. (b): the Ga-bilayer model by Biegelsen et al. [33] which has two Ga-dimers at the top layer and one Ga-dimer at the third layer. (c): the As model proposed by Skala et al. [62]. (d): the model for the 2x6 phase by Biegelsen et al. [33]. Please notice that the notation of the crystal axis in the figure is only for the 4x2 surface, it should be rotated 90° along the (001) axis for the 2x6 surface.

2. Experimental

2.1. General

The experiments were carried out in an ultrahigh vacuum (UHV) FI-STM (field-ion scanning tunneling spectroscope) which was combined with a small commercial MBE system (ULVAC JAPAN, Ltd.) through a 2-3/4" O. D. gate valve (Fig. 4). Portion A in Fig. 4 is the regular FI-STM and the STM set up can be seen through the front 8" O. D. viewing port at the lower FI-STM. Another viewing port to the right is for LEED observations. Portion B is the MBE apparatus housed in a small chamber. There are six Knudsen cells and individual shutters are controlled by a personal computer. The two mechanical feedthroughs, F1 and F2, positioned horizontally with 90° rotated transport the sample between the MBE and STM sections smoothly and quickly without disturbing the UHV conditions. The base pressure of the STM and MBE chambers is 4×10^{-11} and 1×10^{-10} Torr, respectively.

The GaAs(001) sample was cut from on-axis wafers (dopant Si, 1×10^{18} cm^{-3}), chemically etched in a stan-

dard 4:1:1 mixture of H_2SO_4:H_2O_2:DI H_2O and was mounted on the sample holder with indium. The sample was outgassed at 400°C in the MBE chamber overnight. Surface oxides were removed by annealing at 600°C in an As_4 flux [5,6]. The buffer layers were then grown at the growth temperature in the range of 540°C - 630°C, the As_4/Ga flux ratio of ~30, and the growth rate of 0.15mm/h, being monitored by the RHEED intensity oscillation. The Si doping level was calibrated by SIMS (secondary ion mass spectrometry) and kept below $1.5\times10^{18}cm^{-3}$ in the present work, in order to minimize surface kink defects induced by dopants [67]. The quenching of the sample was performed by removing the sample mounted on the small sample holder (Ta made, 3x12x24 mm^3 in size) out of the MBE growth station and transferring to the STM chamber typically in 2 to 3 seconds. We estimate the quenching rate of the sample holder to be approximately 50°C/s by IR thermometer measurements.

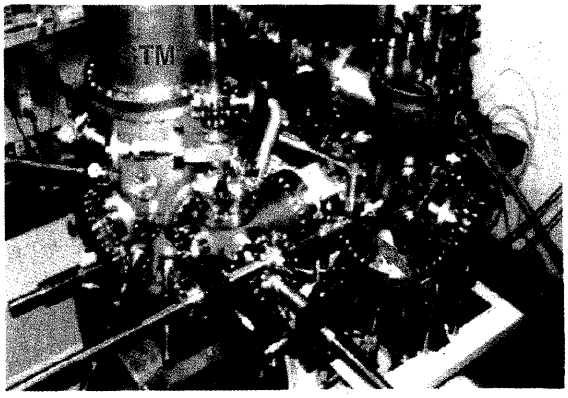

Figure 4. Photograph of the combined MBE-STM apparatus used in this study. A: the FI-STM chamber, B: MBE chamber, F1 and F2: mechanical feedthroughs for sample transfer between A and B. The MBE section is incorporated to the existing FI-STM apparatus.

2.2. RHEED measurement

The RHEED intensity profiles of the (2x4) surface were recorded both during the sample preparation (at elevated temperatures) and after the STM observation (at room temperature) and we found that the spot intensities were essentially the same for both cases, implying that the quenching rate is sufficiently high with the small heat capacitance of the sample holder. The kinetic energy of the electron beam was 10KeV and the angle of incidence was chosen to be 1.6±0.2° in the [$\bar{1}$10] azimuth. FP claimed that they used 0.07° (1.3mrad) to minimize the undesired multiple scattering [14,17]. We question the validity of the claim of FP. The simple relationship between the angle of incidence and the RHEED spots dictates that the angle of incidence has to be larger than at least 1.2° in order to observe the 3/4ths or higher order spots. When the angle of incidence becomes smaller, overlapping of the Ewald sphere with the reciprocal-lattice rods associated with the zero-th Laue zone becomes smaller. Under this situation, we can observe the zero-th Laue zone spots only if the reciprocal-lattice rods have sufficiently broadened width (because of the imperfections of the surface) enough to cross over with the Ewald sphere. Then we cannot reliably analyze the relative intensities of the diffraction spots, since the Ewald sphere is not cutting the center of the reciprocal-lattice rods. The angle of incidence of 1.6° was chosen in the present observations for this reason. (The basic idea can be found in Ref. 66 and in many textbooks on diffraction analysis.)

2.3. Sample preparation of the (2x4) and c(4x4) phases

We have followed the sample preparation method described by FP [14,17] and obtained the 1/4th, 2/4ths and 3/4ths fractional order spot intensity profiles consistent with those described by them, although the details of the RHEED patterns could not be compared since no comprehensive data has been published in the past for the detailed RHEED spot intensities for the α, β and γ phases. The most stable β phase was prepared by annealing the substrate at the growth temperature maintaining the As_4 flux until the 2/4ths intensity grew to the comparable intensity with the 1/4th and 3/4ths intensities. The wide range of growth temperatures (540°C - 630°C) could be used for the β phase.

We have used three different methods to prepare the c(4x4) and (2x4) phases: (I) The α, γ and c(4x4) phases were prepared by annealing the substrate which exhibits the β phase for several minutes at 640°C, 510°C and below 490°C, respectively, maintaining an As_4 flux. Taking into account the high vapor pressure of As, the c(4x4) phase is known to be the most As-rich phase. (II) The γ, β and α phases were also obtained from the c(4x4) phase by heating the substrate at 300°C, 390°C and 460°C, respectively, without the As_4 flux [33]. (III) The migration enhanced epitaxy [68] technique was used as well as the regular MBE growth, mentioned above, where As_4 and Ga are alternately supplied to the substrate (by opening the As and Ga shutters alternately) to enhance the surface migration of Ga much more (~ 10 times) than the case of the regular MBE [68]. We used MEE at the As_4/Ga flux ratio of 20:1 for the c(4x4) and 12:1 for (2x4) γ phase, at the sample temperature of 500°C. We have succeeded to grow the c(4x4) and (2x4)-γ phases, as well as mixed phases by this method [42]. However, compared with the normal MBE, the MEE technique have some shortcomings. They are (1) the decreasing growth rate, and (2) the shorter lifetime for the shutter bellows because of the frequent operation of the shutters. Thus, it is more appropriate for growing a thin material such as superlattice, or just for exploratory research.

Because of the high vapor pressure of As, the temperature of the sample and the As_4/Ga flux ratio critically affect the surface stoichiometry. For instance, the surface is growing and both Ga and As atoms are being supplied to the surface simultaneously in method (I), while the As atoms are continuously desorbing from the

surface in method (II). In the case of method (III), the surface is under the steady-state condition with As_4 flux. In all the methods, there expected significant amounts of mass transfer of As and Ga atoms between the surface and vacuum as well as on the surface. Once the As atoms located on the surface leave the surface for migration, the Ga atoms underneath are then exposed to the vacuum and become highly mobile. Therefore, we expect sufficiently high migration of the As and Ga atoms when the c(4x4) and (2x4) phases are prepared. Therefore, the surface is nearly under steady-state conditions and removing As atoms is essentially equivalent to adding Ga atoms.

2.4. Sample preparation of the Ga-rich 4x2 and 4x6 phases

Once the buffer layer growth was completed, the substrate heating was turned off and the temperatures of As and Ga Knudsen cells were set to an appropriate value to produce a desirable flux necessary for the low temperature MEE growth of a well-defined Ga-rich surfaces at 500°C. Allowing the As and Ga fluxes stabilized at the preset Knudsen-cell temperatures for about one hour, the MEE over-growth at 500°C was started. The choice of the growth temperature of 500°C for MEE is based on the following considerations: First, we have performed a parrell STM study on heteroepitaxial MEE growth of InAs on the GaAs(001) at 500°C with high-quality interfaces [69]. Second, we could proceed the MEE growth with a significantly low As pressure (within 10^{-8} Torr range) at 500°C, compared with usually 10^{-6} - 10^{-5} Torr. Use of a higher As pressure always results in the formation of the As-rich phase. For instance, the Ga-rich layer growth cannot be initiated at the higher As pressure in the most cases even at Ga-shutter opening cycle. Last, under the normal higher growth temperature (~600°C), we have to use the high As pressure and faster shutter switching rate in order to prepare the smooth Ga-rich surface. Otherwise, it also results in the formation of the As-rich surface, whereas decreasing the As or increasing the Ga pressure causes undesirably rough growth-front with too much Ga, such as Ga-droplets. By the low temperature MEE, atomically smooth as-deposited Ga-rich surfaces could be reliably grown by optimizing the As_4/Ga ratio, the As pressure and the switching duration of the shutters and the alternative growth of full monolayer Ga and As can be assured.

When all the expected factors were satisfied, the sample was annealed at 500°C under the As_4 flux until the well-ordered and known 2x4 RHEED pattern appeared. Then typically 12 MEE cycles were grown in order to minimize the effect from the substrate. The sample was transfered to the STM chamber within one second right after the last Ga opening cycle. We have found that As_4/Ga flux ratios of 8 and 6 are preferred for the preparation of the as-deposited 4x2 and "genuine" 4x6 surfaces, respectively, with 2 sec As + 2 sec Ga alternating exposures. For the other "pseudo" 4x6 ("pseudo 4x6") surfaces, a relatively wide range of As_4/Ga flux ratios could be used and the growth condition is more flexible. We have also successfully prepared these surfaces by post-annealing of the 2x4 surface (the details will be discussed in next section). In either case, care was taken to make sure that the data obtained were reliable and reproducible for various reconstructions. The surface was also re-examined by RHEED after the STM scanning.

2.5. STM observation

The STM images were obtained at the sample bias of Vs = -3.5V to -2.0V with respect to the tip (grounded), and a constant tunneling current It = 20-40pA. The scanning area can be in the range of 20Å to 12,000Å in the routine measurement. For the 2x4 surface, we have observed that tunneling into the sample empty states (Vs > 0) is unstable or only gives us a degraded resolution for the As-rich (2x4) phases in contrast to the GaAs(110) surface [70]. This characteristic has noted and been discussed first by Pashley [32]. Keeping a low doping level enhances this effect. Dual bias imaging has used successfully for the Be-doped p-type (2x4) phase by Wassermeier and the effect is attributed to the difference of the Fermi level pinning position and tip-induced band bending [36]. The contribution to the tunneling current (filled states) is attributed to the double occupied lone-pair states located on the As dimers [36,37]. For the Ga-rich 4x2 and 4x6 surfaces, we have successfully obtained the empty states images, the origin will be discussed in details in Section 3.

3. Results and Discussions

3.1. STM images of the (2x4)-α, β and γ phases

Figures 5(a), (b) and (c) show typical gray scale STM images of the (2x4)-α, β and γ phases, respectively, with insets showing the enlarged small area images and the typical depth profile measured along the [110] direction. Bright features are running along the direction with a spacing $d = 4a_0$ (a_0 = 4.0Å: the unit of the GaAs(001)1x1 surface) measured along the [110] direction and are divided into the unit of $2a_0$ in the $[\bar{1}10]$ direction, forming the (2x4) symmetry with a unit size of 8×16Å [32-52]. Dark lines between them are identified to be As dimer vacancy regions as discussed by Pashley [32], supporting the vacancy model of the (2x4) phase [32, 53].

We observe several types of defects as have been discussed previously [32]. They are: (1) complete As dimer vacancies from the (2x4) unit which forms a dark region separated by $2a_0$ along the $[\bar{1}10]$ direction, (2) shift of the (2x4) units by a_0 along the $[\bar{1}10]$ direction, which is responsible for forming the c(2x8) phases, and (3) shift of the (2x4) units by a_0 along the [110] direction, which are called "kink" and forms out-of-phase domain boundary in terms of the 4x symmetry. Defects (1) form the (2x4) units separated by $d = 8a_0$ measured along the [110] direction (see Fig. 5(c) for the definition of d). Those kinks (defects (3)) may form the (2x4) units separated by $d = 3a_0$ and $5a_0$, if the kinks are not aligned along the [110] direction perfectly.

We can clearly see in the STM images, enlarged small

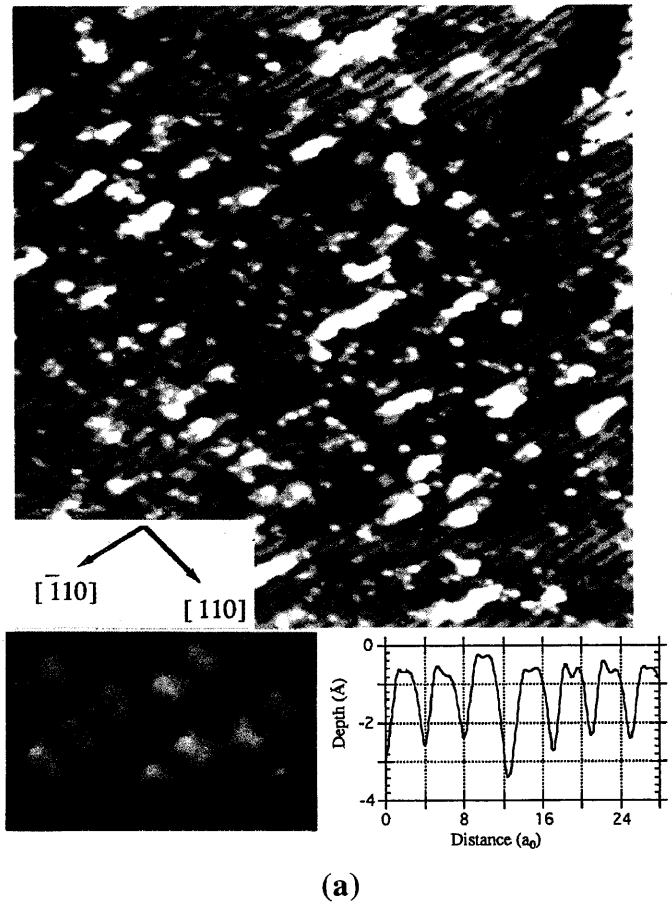

(a)

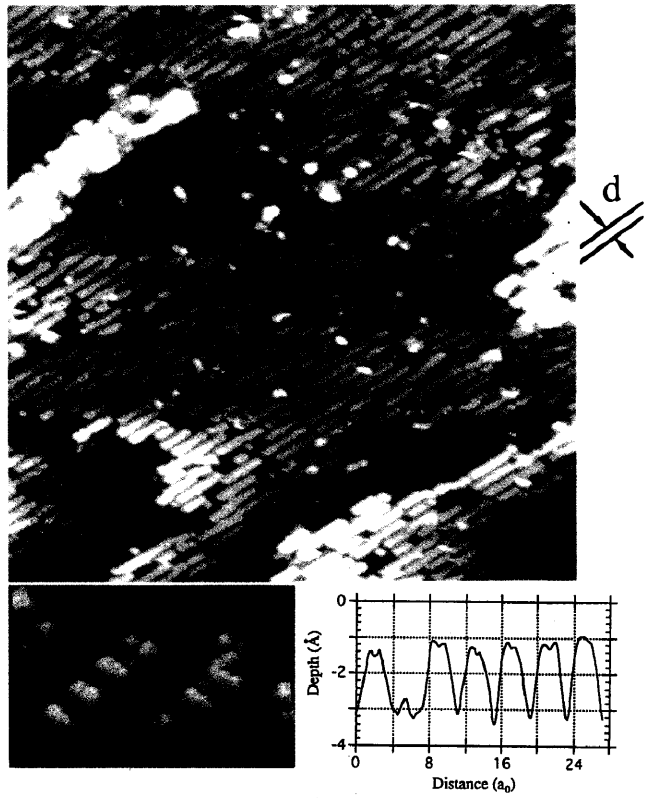

(c)

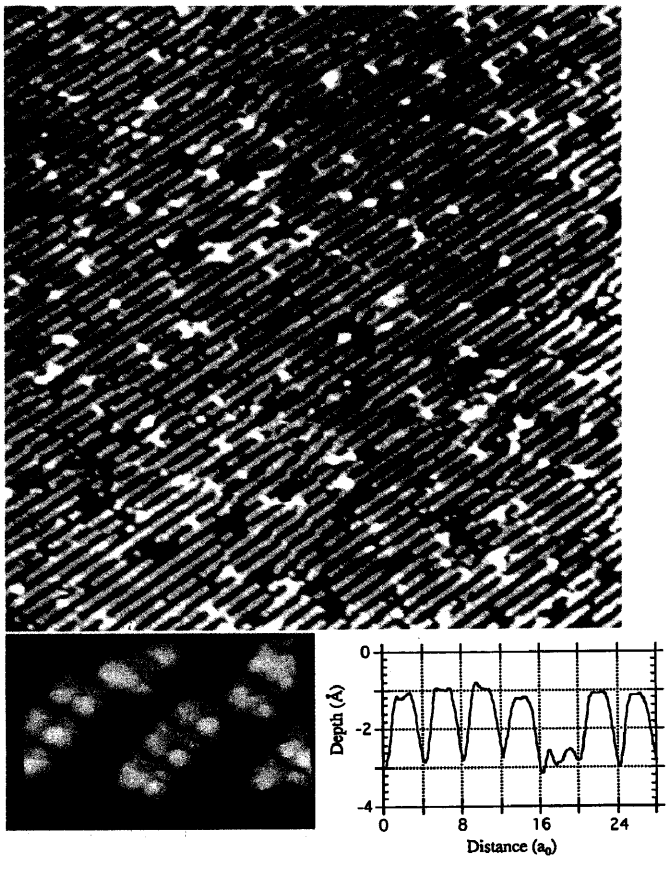

(b)

Figure 5. Typical 3-dimensional display STM images of the (a) α, (b) β and (c) γ phases (800×800Å) together with insets showing the magnified images to show the details and their depth profiles measured along the [110] direction. In the STM images, it is evident that the bright lines are running along the direction, separated typically by $4a_0$ along the [110] direction. All of the (2x4) unit cells of these three phases consist of two As dimers and two dimer vacancies.

area images and contour profiles (Fig. 5) that *the* (2×4) *units at the outermost surface layer of the* α, β *and* γ *phases all consist of two As dimers and two dimer vacancies* [43]. It is interesting to note that the detailed analysis shows that the distance between these two protrusions is not exactly a_0 but approximately 15% larger. Since STM images represent the electronic density of states and not the atomic position itself, this difference suggests that the peak position of the density of states is slightly shifted from the As dimer position in the [110] direction, which is similar to the case calculated by Ohno for the three As-dimer model [55]. This might be part of the reason for the erroneous assignment of the STM images as the three As-dimer model in the past. Another reason may be because some authors measure the full width of the bright imaged As dimers in the [110] direction assuming that the width is proportional to the number of the As dimers in a unit when the resolution of the STM images is not sufficient to resolve the individual As dimers. This procedure is obviously wrong. And the number of the humps and separation of them in a unit must be analyzed for proper interpretation.

We have found a simple rule to interpret the STM im-

ages correctly which can be applied even in the case of rather poor resolution STM images. The rule utilizes a relationship between the number of the As dimer in the (2x4) unit at the outermost surface layer and the kink geometry. The As dimer kink is produced with lateral translation of the unit distance a_0 in the [110] direction. Therefore, the image of As dimers must appear continuous at the kink area, if the (2x4) or c(2x8) unit consists of three As dimers (Figs. 6(a) and (b)), while there should still be a space of a_0 in between these two units if the unit consists of two As dimers (Figs. 6(c) and (d)). Based on this rule and the careful inspection of the kink structures, we can rule out the possibility of the three As-dimer model for the (2x4) phases from the previously published STM images. Indeed, almost all previously published STM data claiming the three As-dimer model fail this test and they should be interpreted correctly in terms of the two As-dimer model.

In the β phase (Fig. 5(b)), the dimer vacancy rows are straight and extend over 300Å along the [$\bar{1}$10] directions in average before any kinks. The kinks tend to align in the [110] direction, forming large domains extending up to 3000Å along the [110] direction, demonstrating a high degree of ordering in the β phase [41]. In the α phase (Fig. 5(a)), the dimer vacancy rows are interrupted by kinks in every several dimer length along the [$\bar{1}$10] direction. These kinks appear to align in the [110] direction, similar to the β phase. The domain size of the α phase is typically 60Å and 500Å in the [$\bar{1}$10] and [110] directions, respectively. In the γ phase, the kink density in the direction is similar to that of the α phase but kinks distribute randomly and do not show any ordering in the [110] direction, unlike the case for the α phase. In the case of the γ phase, there are significant portion of *open areas* , where the As dimers at the outermost surface layer are missing and the underneath terrace structures are exposed. The details will be discussed in section 3.4. The domain size of the γ phase in Fig. 5(c) is approximately 60Å and 100Å in the [$\bar{1}$10] and [110] directions, respectively, which depends on the growth conditions.

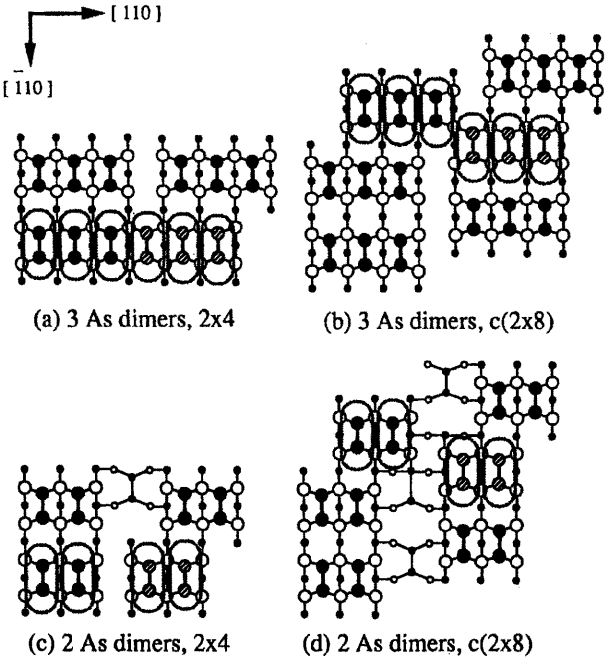

Figure 6. Schematic STM images showing the relationship between the kinks and As dimer arrangements nearby for the 2x4 and c(2x8) phases, based on the two As-dimer and three As-dimer models. If the unit consists of three As dimers, the As dimers make direct contact with the adjacent As dimers at the kink position, while there is always a gap of one As dimer width if the unit consists of two As dimers.

We have examined the distribution of the separation of the neighbouring (2x4) units d measured in the [110] direction. For the β phase, the nominal separation of d = $4a_0$ is dominant (98%) with small fractions of $3a_0$ (<1%) and $5a_0$ (<1%). For the α phase, the result is similar to the β phase with slightly higher fractions for both $3a_0$ (8%) and $5a_0$ (4%), implying the slightly higher kink density compared with the β phase. For the γ phase, the distribution of d varies greatly depending on the detailed sample preparation conditions. The distribution of d for the case of the surface shown in Fig. 5(c) is $4a_0$ (63%), $7a_0$ (15%), $3a_0$ (8%), $5a_0$ (3%) and > $7a_0$ (11%). This result shows that the γ phase is characterized by a small size of the (2x4) phase which are separated with the *open area* typically with d = $7a_0$.

Detailed quantitative analysis of the STM data can yield useful information on the sub-surface structures. The depth profiles of the STM images measured in the [110] direction for the α, β and γ phases show distinct differences between the α and β (γ) phases. Typically, we do not see any structure between the dimers in the α phase (the depth profile of Fig. 5(a)), while we regularly observe one or two faint line protrusions in the vacancy region of the β (γ) phases (the depth profiles of Figs. 5(b) and (c)). Figure 7 summarizes the depth profile in the As dimer vacancy measured from the position of As dimers at the outermost surface layer as a function of separation d of the neighboring (2x4) units (in unit of a_0). The measured depth for the regular (2x4) region, d = $4a_0$, is 2.1±0.3Å for all the α, β and γ phases. This measured value is smaller than the expected value of 2.8Å = h, the bilayer depth of the GaAs(001) surface. We interpret this as a tip effect, namely the depth to width ratio of the vacancy region is too large to image the bottom. However, in the case of the separation d >$5a_0$, we observe the reasonable depth in the α phase, which is approximately 2.8Å = h, while the depth in the β (γ) phase is about 1.4Å one half of the bilayer depth ($1/2h$).

Since we are imaging the filled density of states, we

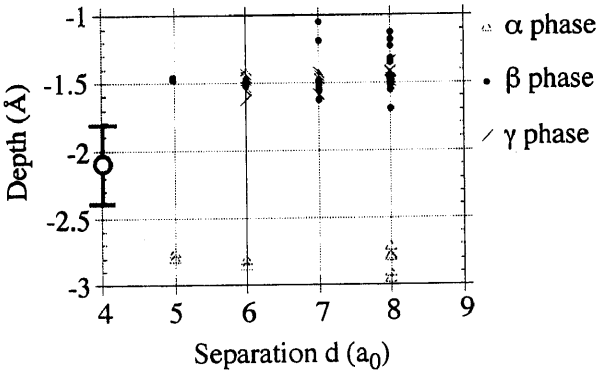

Figure 7. Plot of the depth height of the dimer vacancy region for three different phases, measured from the position of the top layer As dimers as a function of the separation d (in unit of a0).

are observing the As atoms as protrusion and the dangling bonds of Ga atoms are not be imaged. When we examine the models of (2x4) phases shown in Fig. 2, no structure should produce the depth height of $1/2h$ at the As vacancy regions. Thus the observation of the $1/2h$ depth for the β and γ phases in Fig. 7 implies that there must be some unknown subsurface structure in the vacancy region for the case of the β and γ phases. This observation provides us with sufficient information to discuss the subsurface structures.

3.2. Dynamical RHEED analysis of the (2x4)-α, β and γ phases

In order to fully understand the structures of the α, β and γ phases, we have calculated the RHEED spot intensities for the possible (2x4) models using the dynamical theory developed by Ichimiya [65]. Although it has been known that the dynamical effect is very important for the analysis of the GaAs(001) surface [12], a systematic analysis using dynamical RHEED calculation has never been performed, most likely due to the lack of detailed knowledge of the surface structure [43].

In the present calculation, nineteen beams in the zero-th Laue zone of the [$\bar{1}$10] incidence were taken into account. As the RHEED intensities in the zero-th Laue zone are insensitive to the displacement lateral to the incident direction, relaxations along the [$\bar{1}$10] direction are not taken into account [65].

Basic structure models we used for the analysis are described in Figs. 2(a) through (f). In general, we have assumed that the As dimers are contracted by 0.2Å perpendicular to the surface in order to form dimer without changing the As-Ga bond length and have no displacement along the [110] direction. Other atoms were assumed to have no relaxation from the bulk positions. We also examined the influence of the small displacement of the atom positions to the spot intensities. The rocking curves for the five zero-th order Laue zone reflections (0 0), (0 1/4), (0 1/2), (0 3/4) and (0 1) were calculated and the spot intensities were obtained by averaging over the incidence angle of $\pm$ 0.2°.

One set of the RHEED intensity rocking curves for the

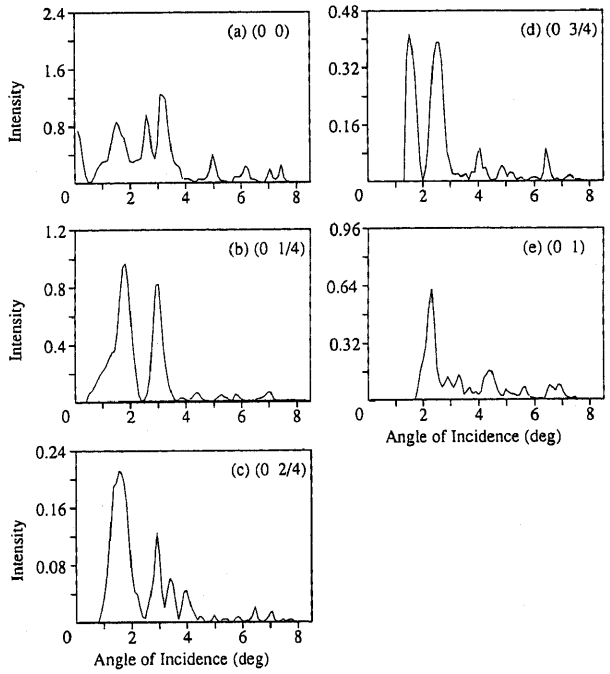

Figure 8. The calculated rocking curves for (a): (0 0) spot , (b): (0 1/4) spot , (c): (0 2/4) spot , (d): (0 3/4) spot and (e): (0 1) spot for the Chadi's two As dimer model (Fig. 2(b)).

case of the Chadi's two As-dimer model are reproduced here, in order to demonstrate the full extent of our dynamical calculation (Fig. 8). The parameters used for this model in the dynamical calculation are shown in Fig. 9. These rocking curves are in good agreement with the current experiment (10keV), as well as those obtained by P. K. Lasen et al. [71], although there are some angle shifts due to the energy difference between their experiment (12.5keV) and ours. We wish to point out that small changes of these parameters do not produce significant changes in the relative values of the spot intensities. Furthermore, it is clearly demonstrated here that the incident angle must be larger than 0.8° to observe the 2/4ths feature and than 1.3° to observe the 3/4ths feature at all, once again disproving the FP's claim on the small angle of incidence. The fully detailed account of the RHEED calculation will be published elsewhere [72].

In order to qualitatively compare the theory and experiment, we used a photo multiplier with pin-point fiber optics to measure the RHEED spot intensities. The observed RHEED patterns taken at room temperature are plotted in Fig. 10 (a), (b) and (c) for the α, β and γ phases, respectively, corresponding the STM images in Fig. 5. They were then de-broadened to compare with the theoretical results and are plotted in Fig. 10 (d), (e) and (f) for the α, β and γ phases, respectively. We confirm the characteristic features in the RHEED spot intensities as reported by FP [14,17]. The 2/4ths feature is weak for the α phase and for the β phase relatively strong with respect to the 1/4th and 3/4ths intensities. It is almost absent for the γ phase.

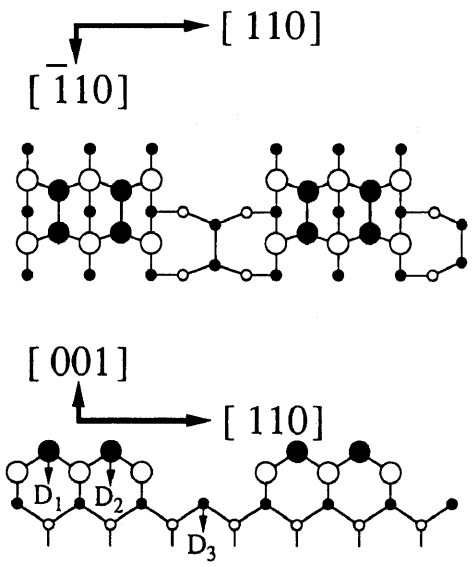

Figure 9. Parameters used for the Chadi's two As dimer model (Fig. 2 (b)) for the dynamical RHEED calculation. Contractions of the As dimers (two on the top layer and one at the third layer) are all the same 0.2A.

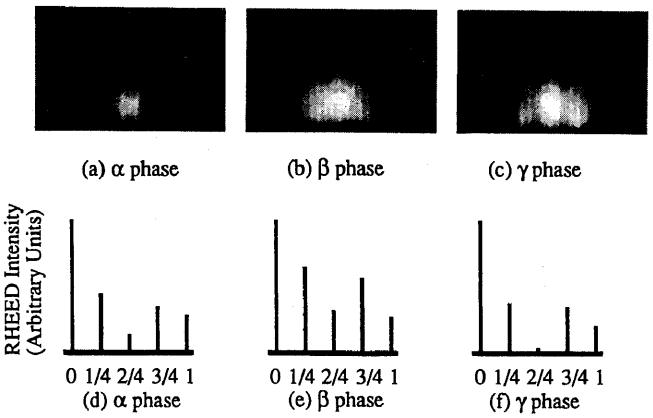

Figure 10. Experimental RHEED patterns for the (a) α, (b) β and (c) γ phases and their debroadened spot intensity profiles for (d) α, (e) β and (f) γ phases. The results are in good agreement with the description by FP[14,17].

The results of calculated spot intensities are summarized in Fig. 11. For the case of two As-dimer model by Chadi (Fig. 2(b)), we have calculated for both (b1) without relaxation and (b2) with relaxation calculated by NF [57]. For the case of the two As-dimer model for the α phase proposed by FP [14,17], we have calculated for the cases of (c) without second layer Ga dimerization or relaxation, proposed by Chadi (Fig. 2(c)) [54] with the second layer Ga dimerization but without relaxation, by FP (Fig. 2(d)) [14,17], and (e) after full relaxation by NF (Fig. 2(e)) [56]. We also show the result of the kinematical calculation for this model taking second layer into account (Fig. 11(g)).

The three As-dimer model, proposed by Chadi (Fig. 2(a)), gives a weak intensity for the 3/4ths fractional order spot (Fig. 11(a)), in contrast to the result by kinematical calculation [14,17]. We do not find the noticeable changes by varying the contraction of the As dimers from -0.4Å to -0.05Å. The inward relaxation of the second layer Ga atoms having dangling bonds (up to 0.8Å) yields weak intensity for 1/4th and 2/4th spot intensities and does not agree with the experiment. *More importantly, the three As dimer unit is not consistent with our STM images of the α, β or γ phase (Fig. 5).*

McCoy et al. have analyzed the (2x4) unit structure by fitting the experimental rocking curves with the calculated ones using the dynamical RHEED theory [62]. They used the Chadi's three As-dimer unit (Fig. 4(a)) and allowed the relaxation of the first and second layer atoms to achieve the best fit of the rocking curves. They concluded that the center As dimer is contracted by 0.2Å perpendicular to the surface (rumpling) and the second layer Ga atoms have both in-plane and perpendicular relaxation [62]. They claimed that the rumpling agrees with the STM observation by Gallagher et al [37]. However, the separation between two protrusions Gallagher et al. observed in their high resolution STM images can be measured to be approximately 5Å although they are not explicitly stating the value in their paper. The separation of the two protrusions is $2a_0$ = 8.0Å expected from the rumpling McCoy et al. claimed[62] but it does not agree with the STM observation. In their dynamical analysis, McCoy et al. used the normalized curves to fit each fractional order spot, neglecting the absolute value of spot intensity [62]. Although the normalized intensities and intensity peak positions of their fitted rocking curves agree well with the experimental curves, the spot intensities using their fitted atom positions are similar the results obtained for Chadi's three As-dimer unit without relaxation (Fig. 2(a)). Main difference is that their coordinates yield only one quarter of intensity for the 2/4th spot comparing with the one for Chadi's model (Fig. 11(a)). This is one of the confusions we have been discussing in Section I and trying to resolve. The extra As-dimer model by FP [14,17] (Fig. 2(f)) gives the weak 3/4ths spot intensity, similar to the case of the three-dimer model (Fig. 2(a)) and does not agree with any experimental results.

The two As-dimer model proposed by Chadi (Fig. 2(b)), gives a nearly equal intensity of the 1/4th, 2/4ths and 3/4ths fractional order spots (Fig. 11(b1)) and are consistent with the β phase (Fig. 10(b)). Changing the contraction of the As dimers from -0.4Å to -0.05Å results in approximately 20% variation of the zero-th spot intensity and the best fit to the experiment is obtained at the contraction value of approximately -0.2Å . The kinematical calculation for this model, taking only the first layer into account, produces the same results with two As dimer model discussed by FP [14,17], namely zero intensity for the 2/4ths spot intensity. However, since they are only three out of four pairs of Ga atoms in the second layer, an interference effect is expected between the diffractions from the first and second layers and the intensity of the reciprocal lattice rods oscillate sinusoidally as a function of reciprocal lattice coordinate

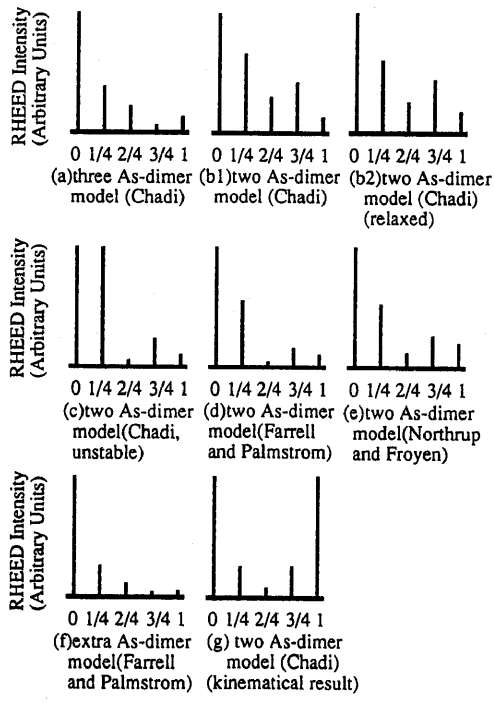

Figure 11. Calculated RHEED spot intensity profiles for various models (a) to (f) using the dynamical theory being discussed in this text. (g) is based on the kinematical calculation

normal to the surface (kz) [73]. If we consider the case of a less ordered surface, the intensity of the reciprocal lattice rod should be averaged and we obtain the spot intensities shown in Fig. 11(g). The averaged spot intensities for the (0 0), (0 1/4), (0 1/2), (0 3/4) and (0 1) spots by the kinematical calculation for the Chadi's two As-dimer model are 13, 3, 1, 3, 13, respectively (Fig. 11(g)); as the sum of the spot intensities calculated kinematically for the two As-dimer unit (4, 2, 0, 2, 4) and the three As-dimer unit (9, 1, 1, 1, 9). As a result, we observe non-zero 2/4ths spot intensity even for the kinematical calculation for the Chadi's two As-dimer unit. The dynamical effect further enhances the 2/4ths spot intensity, resulting in a good agreement with the β phase data (Figs. 10(b) and (e)).

NF recently extended their first principle calculation to the Chadi's two As-dimer model [56,57]. We have also calculated the spot intensities based on the detailed coordinates calculated by NF [56,57]. The result is shown in Fig. 11(b2). We do not observe significant differences from the original model (Fig. 11(b1)) and find that the present method is not sensitive with the exact coordinates of the individual atoms but mainly determined by the overall arrangement of the atoms of each atomic layers. We are able to compare the calculated rocking curves with those obtained experimentally by McCoy et. al [62]. We obtain a good agreement in the peak positions of the rocking curves as well as the absolute value of the spot intensities without significant relaxation. The full accounts of the dynamical RHEED investigations of the GaAs (001)-(2x4) phase will be published elsewhere [72].

Various two As-dimer models with four pairs of Ga atoms in the second layer, proposed by Chadi (Fig. 11(c)) [53], FP (Fig. 11(d)) [14,17], and NF (Fig. 11(e)) [56] yield a weak intensity 2/4ths fractional order spot in general, which is consistent with that of the α phase (Figs. 10(a) and (d)). Although the 2/4ths spot intensity is almost absent for all the cases, the 1/4th spot intensity is sensitive to the dimerization of the two Ga atoms in the second layer (Figs. 11(c) and (d)). By changing the distance of Ga atoms from 4.0Å (Fig. 11(c)) [53] to 3.9Å, the 1/4th spot intensity changes from 1 to 1/4 relative to the zero-th spot intensity. Since the spot intensities are not so sensitive to the relaxation (except for the dimerization) of the second layer Ga atoms, the difference between the FP (Fig. 11(d)) [14,17] and NF (Fig. 11(e)) [56] units may not be discussed based simply on the spot intensity analysis and must involve the detailed analysis of the rocking curves [72]. However, we weigh the theoretical calculations by NF and thus prefer the NF model. Another reason is that the model by NF appears to enable us to explain better the MEIS experiment by Falta et al [31], which will be discussed in section 3-4. The present assignment for the α and β phases is also consistent with the depth profile measurement shown in Fig. 7.

In the case of the γ phase where individual domains are small and are separated typically by d = 7a0, the kinematical calculation can be justified, due to the diminishing dynamic effect, and the RHEED pattern should yield the diminishing 2/4ths fractional order spot (Fig. 11(g)) and indeed agrees well with spot intensities (Fig. 11(c)).

Recently, the disordering (high density of kinks) of the γ phase has been studied by another detailed STM study and total energy calculation [50], in order to clarify the mechanism of this disordering. It is pointed out that the ideal β phase has vacant second layer Ga sites which are potential sites for adsorption of any incident species. The preparation of the 2x4 surface under more As-rich conditions results in the adsorption of As on the surface by occupation of these sites. This seems to have resolved the problem although further evidence is still lack.

Based on these STM and RHEED results, we propose the structure models of the α, β and γ phases as follows. The α phase is two As-dimer model proposed by NF (Fig. 2(e)) [56], the β phase is two As-dimer model proposed by Chadi (Fig. 2(b)) [53] and the γ phase is the locally ordered β phase.

3.3. Transition from the c(4x4) to (2x4)-γ phase

In order to analyze the detailed structure of the open area in the (2x4)-γ phase, we grew the c(4x4) and (2x4)-γ phases, as well as their mixed phases using the migration enhanced epitaxy (MEE) [68]. This method devised by Horikoshi et al. [68] have the following advantages: (1) surface migration of Ga is enhanced much more than the case of the regular MBE and the surface topography is smooth enough to observe the atomic structure by STM even right after quenching the sample just after

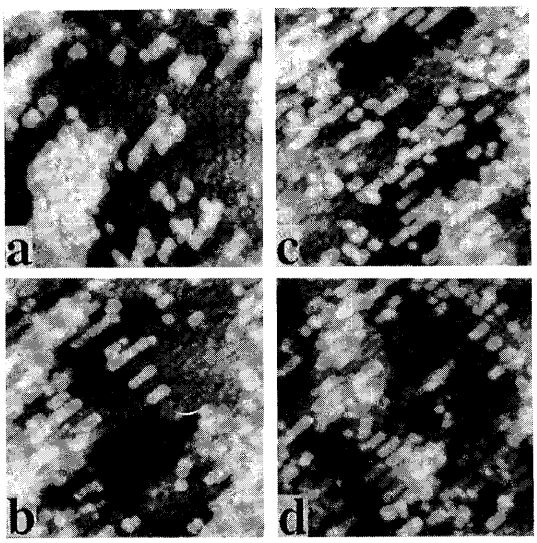

Figure 12. A series of the STM images taken for the study of the transition from the most As-rich c(4x4) phase to the γ phase making a good use of the MEE advantage of controlling the surface stoichiometry. The As_4/Ga flux ratio is (a): 20:1, (b):18:1, (c):17:1, and (d): 15:1.

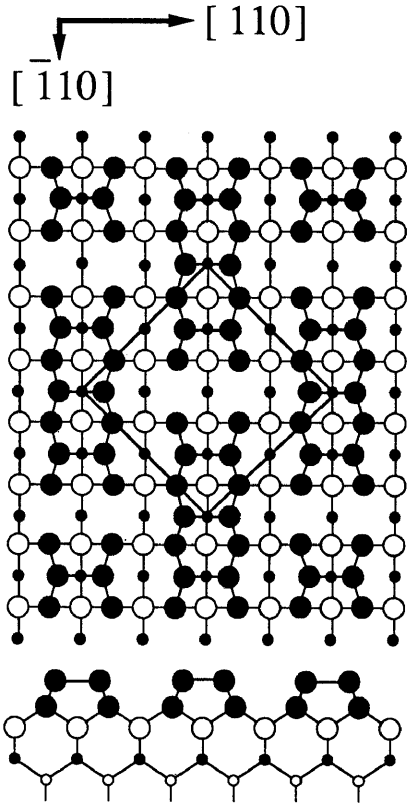

Figure 13. Schematic of the c(4x4) phase proposed by Biegelsen et al. [33].

growth [69], (2) the surface stoichiometry can be controlled easily by changing the As and Ga shutter opening durations [66]. Figure 12 shows the surface changes as we increase the As_4/Ga flux ratio from 20:1 for the c(4x4) (Fig. 12(a)) to 15:1 for the mixture of the c(4x4) and γ phase (Fig. 12(d)), at the sample temperature of 500°C. Similarly, we could obtain the (2x4)-γ phase at the As_4/Ga flux ratio from 12:1.

The STM image in Fig. 12(a) is typical for the c(4x4) phase. The unit has the periodicity of $4a_0$ and $2a_0$ in the [$\bar{1}$10] and [110] directions, respectively, forming the c(4x4) symmetry. The structure model for the c(4x4) proposed by Biegelsen et al. [33] and accepted by many authors is shown in Fig. 13. This model consists of three As dimers on the As atoms in a c(4x4) unit forming the As double layer. In order to compare our data with the model, we plotted the depth profile of the c(4x4) phase along the [$\bar{1}$10] and [110] directions in Figs. 14(a) and (b), respectively. Figure 14(c) shows the depth profile of the (2x4)-γ (β) phase for comparison. The protrusions observed by STM along the [$\bar{1}$10] direction show two peaks (not three) separated by $2a_0$, which is consistent with the model by Biegelsen et al. [33] realizing the enhanced electronic density of states at the corner As dimers. The periodicity of the protrusions in the depth profile along the [110] direction is consistent with the model.

Based on these STM analyses, we confirm the structure model proposed by Biegelsen et al. for the c(4x4) phase [33]. We note that the ordering of the c(4x4) phase is not perfect [43] and the number of As dimers can be two or even one per unit, similar to the missing dimer defects in the case of the (2x4) phases, and also, we observe the As dimers which are shifted by a_0 towards the [110] direction, similar to the kink defects in the (2x4) phase. By varying the number of As dimers in a unit cell, this model can readily explain experimental results observed by x-ray diffraction [61]. We also observe the local p(2x2) area with two As dimers in a unit, which was first reported by Biegelsen et al [33].

If we compare the image width of the dimers along the dimerization direction between the c(4x4) (Fig. 14(b)) and (2x4) (Fig. 14(c)) phases, we see that the As dimers in the c(4x4) are narrower than those in the (2x4) phase. This results in the marked difference in the STM image between the As dimers in the c(4x4) phase and those in the (2x4) phase: the former is imaged to be small round protrusions, while the latter is of the ordinary oblong shape. We believe that the difference in the chemical surroundings of As dimers in the c(4x4) phase and those in the (2x4) phase is responsible to the difference of the spatial distribution of the dangling bond electronic states and thus result in the significantly different STM images. We also note that the As dimers in the c(4x4) phase are bonded to the As atoms and there is no charge transfer expected from the second layer to the first layer, producing the neutral As dimers on the surface. In contrast, the As dimers in the (2x4) phase are bonded to the Ga atoms and charge transfer from the second layer is expected, resulting in the charged up As dimers. The difference in the electronic density of states has been observed and discussed by Larsen et al. in their UPS study [25]. They have observed a shallower and larger surface states peak for the (2x4) phase than c(4x4) phase, which appears to be consistent with the STM image size difference between the As dimers in the γ (β) and c(4x4) phase. Unfortunately, there has not been theoretical cal-

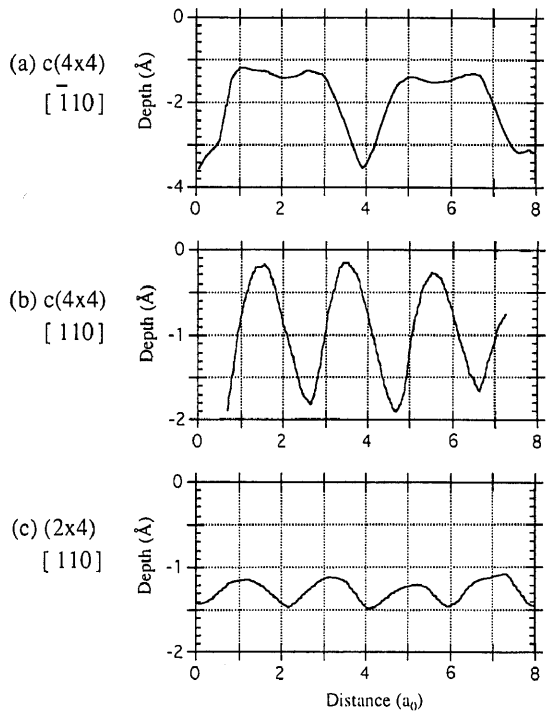

Figure 14. Plots of height profile for (a): c(4x4) in the direction, (b):c(4x4) in the [110] direction and (c): (2x4) in the [110] direction.

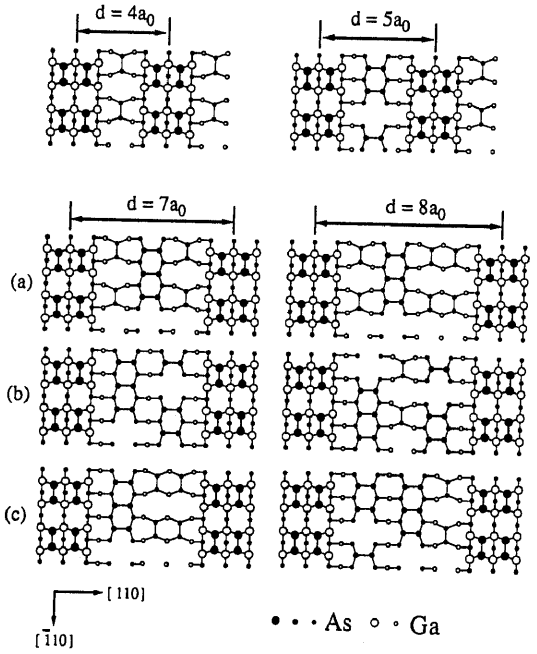

Figure 15. Schematic representation of possible atomic structures of the open areas observed for the γ phase. The faint line structures being observed in the darkly imaged open areas are made of As double layer: the building block of the c(4x4) phase.

culation showing the mapping of density of states from which we can discuss the details of the STM image difference.

After understanding the difference of the STM image between As dimers in the c(4x4) unit and those in the (2x4) unit, it is straightforward to understand the process of the c(4x4) phase transferring to the (2x4)-γ phase under lesser As conditions. Even in the c(4x4) phase, there are islands nucleated with the (2x4) unit structure (Fig. 12(a)). When the slightly less As-rich condition is used, we observe more areas with the (2x4) unit compared with Fig. 12(a) (Fig. 12(b) to (d)). A series of MEE experiments with different As_4/Ga flux ratios show that the (2x4) area becomes dominant with the decreasing As_4/Ga flux ratio and finally the surface becomes identical to the γ phase grown by MBE (Fig. 5(c)) at the As_4/Ga flux ratio of 12:1. In between the nucleated islands of the (2x4) phase, we still see the remaining c(4x4) phase (Fig. 12). These observations naturally lead to the conclusion that the (2x4)-γ phase is formed by replacing the c(4x4) units with the (2x4) units under the less-As conditions. Actually, if we examine the open areas in the γ phase, we frequently observe the subsurface structures and the depth of those are measured to be approximately 1.4Å (= $1/2h$), which is shown in Fig. 5(b) and also is shown systematically in Fig. 7. Thus we conclude that in the open area of the γ phase there are the remaining As dimers on the third layer As atoms, similar to the As double layer of the c(4x4) phase.

We have studied the possible structures of the open area of the γ phase for the separation d = $5a_0$, $7a_0$, and $8a_0$. Figure 15 presents the structure models for those we identified based on the STM data. The abundance of the individual structures varies depending on the preparation conditions. We find that the structure (a) is most abundant (>90%) for the case of d = 7a0, for example.

3.4. Structure model for the (2x4)-α, β, and γ phases

Based on the STM observations and dynamical calculation of the RHEED spot intensities, we propose the following unified model for the (2x4)-α, β, and γ phases (Fig. 16): The α phase is the two As-dimer model proposed by FP [14,17] with relaxation incorporated by NF [56]. The β phase is two As-dimer model proposed by Chadi [53]. The γ phase is merely a mixture of the β phase and the c(4x4) phase.

In all the methods we used for preparing the surface (section 2), we expect significant amounts of mass transfer of As atoms between the surface and vacuum as well as on the surface. Therefore, the surface is nearly under steady-state conditions and removing As atoms is essentially equivalent to adding Ga atoms. For the case of the γ phase, the open area with the local double layer of As has the As coverage up to 1.75ML, the same as that of c(4x4) and the (2x4) region has the As coverage of 0.75ML (one As dimer per unit in the third layer). Thus the γ phase, the mixture phase of the c(4x4) and (2x4)-γ phases, can exhibits the As surface coverage between 1.75ML and 0.75ML. Once the sample preparation condition is chosen, the surface stoichiometry and the domain ratio of the c(4x4) and (2x4)-γ phases are determined. The surface coverage of As of the (2x4)-α, β, γ and c(4x4) phases are 0.5ML, 0.75ML, typically 1ML, and 1.75ML, respectively. This agrees very well

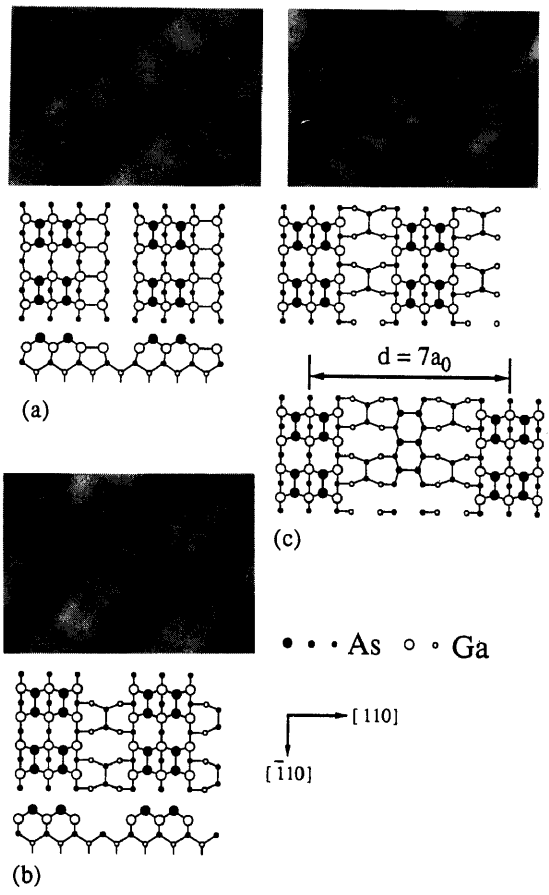

Figure 16. Typical STM images and proposed structure models for the (a) α, (b) β and (c) typical γ phases.

with the previous results.

The unified model proposed here for the c(4x4) and (2x4)-α, β and γ phases may explain the most recent MEIS results by Falta et al. [31] by considering the fact that the Ga atoms exposed to the surface increase in the order from the c(4x4) to γ, β and to α phase, successively. The disagreement Falta et al. pointed out, regarding with the As top layer models, concerns the absolute value in the As/Ga intensity ratio for the (2x4)-α phase [31]. However, in the NF's two As-dimer model of the α phase, all the first layer As dimers, the second layer Ga and the third layer As atoms are shifted from the original positions, therefore, should reduce the blocking of the scattering intensity from the sixth layer Ga atoms which increases the Ga intensity especially at the slightly off of the blocking angle and resolve the intriguing discrepancy.

Now we turn to the Ga-rich phases. A series of STM images of all GaAs(001) Ga-rich phases accessible by our techniques are shown in Fig. 17 and Fig. 18, as a function of surface As coverage for summary understanding of their structural features. The STM images of Fig. 17 were obtained from the as-deposited surfaces by using decreasing As_4/Ga flux ratio during MEE at constant 500°C growth temperature, whereas those in Fig. 18 were prepared by UHV heating with increasing annealing temperatures. According to these preparation processes, the surface Ga coverage should increase from (a) to (h) for both Fig. 17 and Fig. 18. Although the geometrical structures and electronic properties of these surfaces are all inter-connected, the results and discussion in the remainder of this paper are presented for the individual surface reconstruction one at a time, in the order of the 4x2, 2x6, "genuine 4x6", "pseudo 4x6" and 4x1 phases.

3.5. Ga-rich 4x2 reconstruction

The 4x2 phase is known to be the most prominent high temperature phase encountered in the MBE growth and to be most difficult to achieve at room temperature. The corresponding STM images for the as-grown and annealed surfaces are shown in Fig. 17(e) and Fig. 18(e), respectively, where a large atomically flat surface covering an area of at least 900×900Å^2 forms with a smooth bilayer step (H=2.8Å) of the GaAs. The two previous work [33,61] has shown that preparation of the defect-free surface is rather difficult, and both of these groups indeed could not obtain the surface as good as shown in Fig. 17(e) and Fig. 18(e). This difficulty infers that this phase probably has a very narrow composition range with which the structure can be stabilized. This hypothesis is further supported by two other independent experiments on this surface [14,17, 74]. Unlike the case of the As-rich 2x4 surface where the 2/4th fractional diffraction feature can be used to discuss the detailed structural differences [43], there is no characteristic RHEED specular beam intensity behavior which can be used for fingerprint [14,17]. This was also suggested by the soft x-ray photoemission study by Vitomirov et al.[74], where the measured As/Ga 3d core-level intensity ratio remained constant with the 4x2 surface. We should mention that the surface shown in Fig. 17 (e) and Fig.18. (e) reflects the ideally defect-free surfaces case. The usual surface prepared by these techniques exhibits a great number of defects, locally structureless As adsorbates and medium-size Ga clusters. Since these localized features cannot be analyzed and are averaged over a large surface area by conventional composition analysis techniques, there existed no consistent results in the past as for the surface stoichiometry of the 4x2 phase [7-9,12,20,64]. However, what we can speculate at this stage based on the results is that the structure of the 4x2 phase may not be too complicated, unlike the case of the 2x4 surface; a well-defined single domain atomic arrangement should be able to account for this surface layer.

Also as shown in Fig. 17(e), there are only three terraces over such a large area, although the growth temperature is low. This is a clear demonstration of the advantageous MEE effect on surface morphology improvement [42], a great potential for device applications. Compared with the annealed surface where the two-dimensional islands are elongated along the [1̄10] direction (Fig. 17(e)), the islands in Fig. 18(e) appear to be more isotropic and has comparatively smooth edges for both type A and type B steps. These observations certainly reflect the dynamics and kinetics of growth or their competition, and are qualitatively consistent with

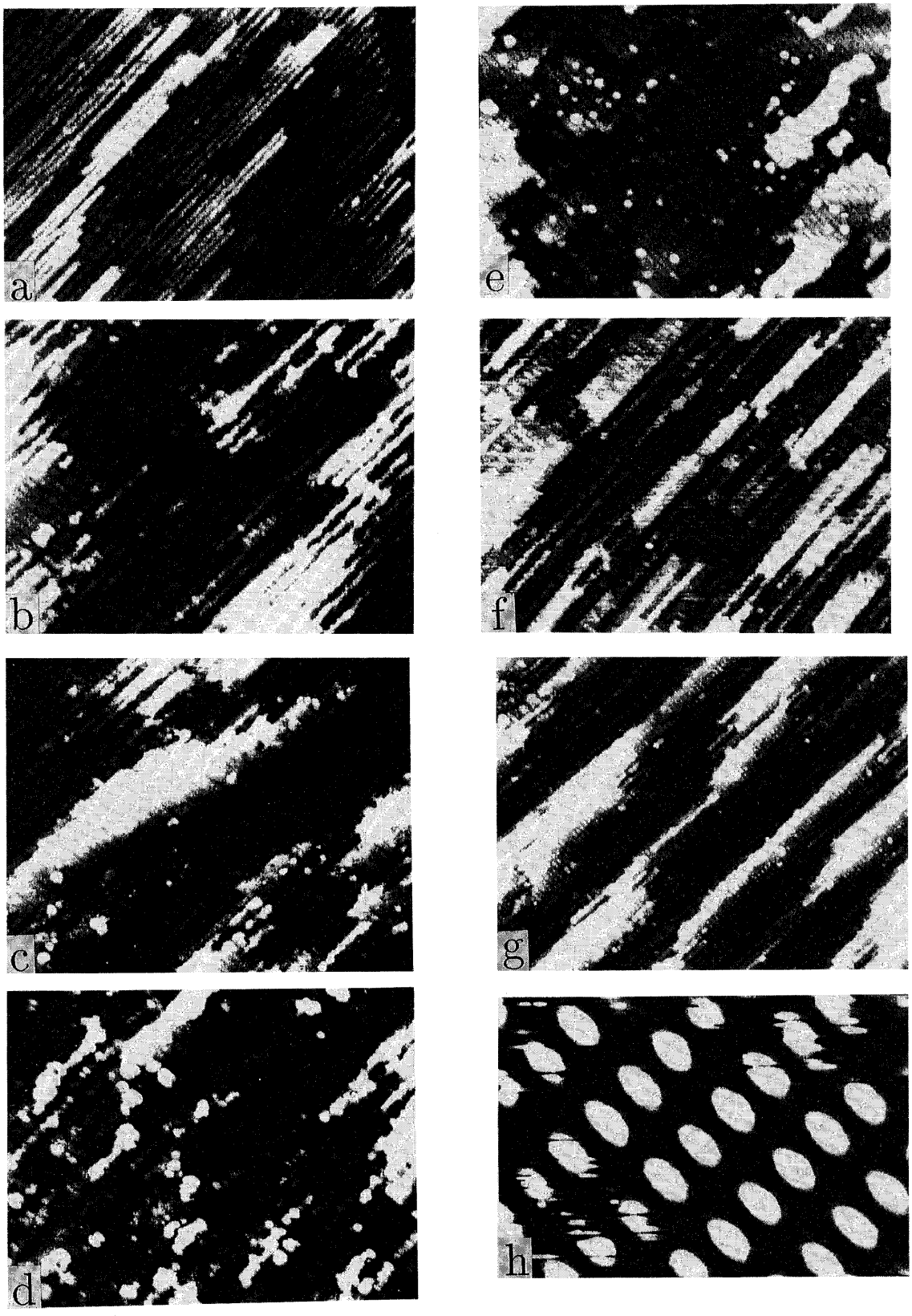

Figure 17. A series of the filled states STM images obtained from the as-deposited Ga-rich surfaces prepared by MEE at 500°C using various As/Ga flux (beam equivalent pressure) ratios (P) and shutter opening times (T_{Ga} and T_{As}). (a): the 2x6 surface (1300×1240Å). P=10, T_{Ga}= T_{As}=2s. (b): the 2x6+4x2 surface (840×850Å). P=10, T_{Ga}=3, T_{As}=2s. (c): the 2x6+4x2 surface (840×850Å). P=9, T_{Ga}=3s, T_{As}=2s. (d): the 2x6+4x2 surface (680×680Å). P=9, T_{Ga}= T_{As}=1s. (e): the 4x2 surface (900×900Å). P=8, T_{Ga}= T_{As}=2s. (f): the 2x6+"genuine" 4x6 surface (710×690Å). P=8, T_{Ga}=3s, T_{As}=2s. (g): the "genuine" 4x6 surface (900×850Å). P=6, T_{Ga}= T_{As}=2s. and (h): the close-up view of the "genuine" 4x6 surface (80×45Å). P=6, T_{Ga}= T_{As}=2s. All images are for the filled states. For all the STM images shown in Fig. 17 and Fig. 18, the [110] direction runs from the lower right corner to the upper left corner, while the [$\bar{1}$10] direction from the lower left corner to the upper right corner.

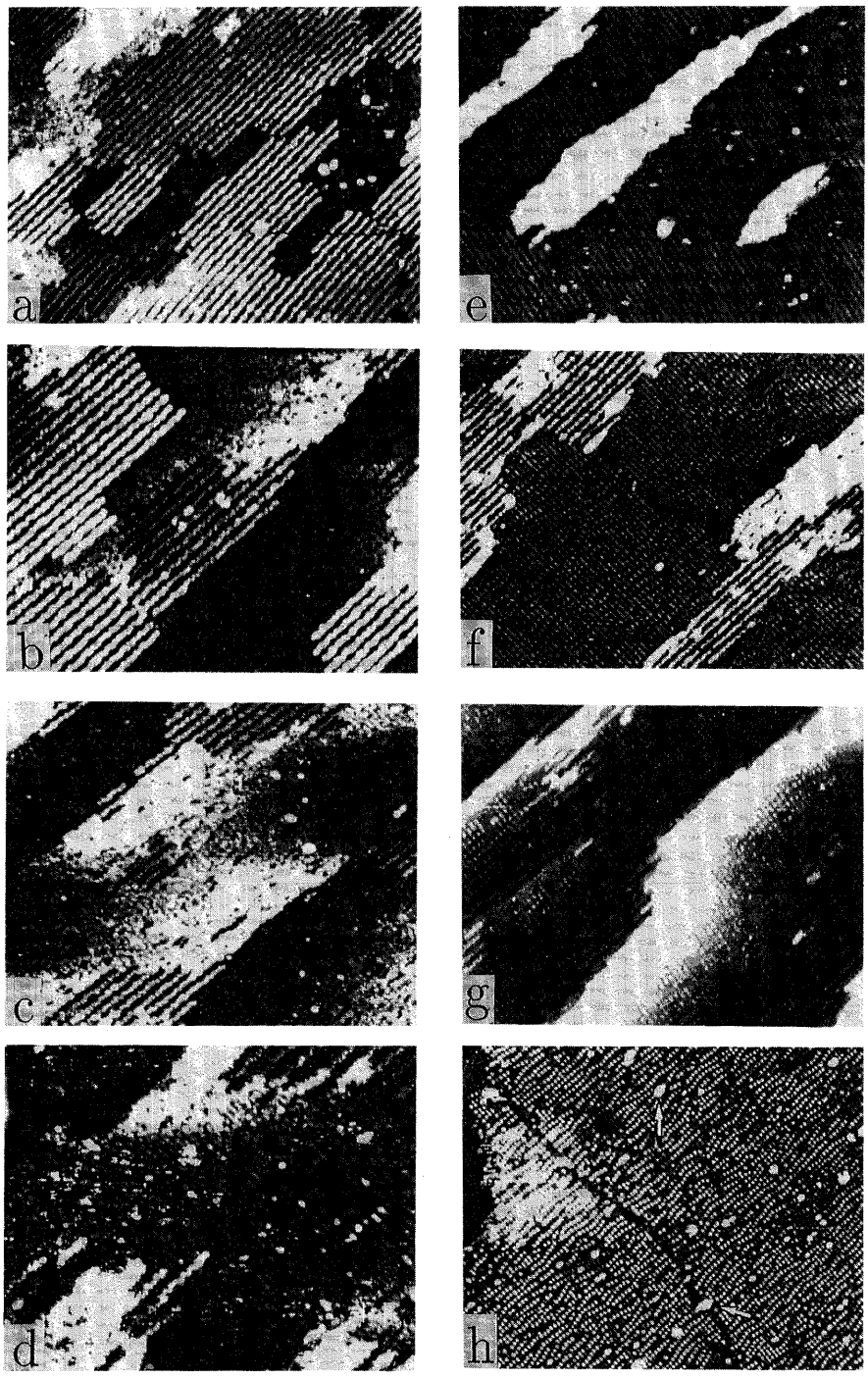

Figure 18. A series of the filled states STM images obtained from the Ga-rich surfaces prepared by UHV annealing of the 2x4 (a) or 2x6 (others) phase with increasing temperatures. (a): the 2x6 surface (540×740Å); 550°C for 20 min. (b): 2x6+disordered(D) (900×940Å); 550°C for 20 min. (c): 2x6+D (900×970Å); 575°C for 10 min. (d): 4x2+D (600×840Å); 575°C for 25 min. (e): pristine 4x2 (1050×800Å); 590°C for 15 min. (f): 2x6+G4x6 (1260×1200Å); 600°C for 10 min. (g):G4x6 (1250×1200Å); 600°C for 20 min. and (h): 4x1 (1700×1650Å); 600°C for 35 min.

the observation on the GaAs(001)2x4 surface by Heller and Lagally [35]. Since it was obtained by prolonging annealing, these islands' shape should be more closely related to that of the equilibrium states. We attempted to make an estimate on the aspect ratio of these islands; hence some thermodynamical information. Unfortunately the degraded tip conditions, mainly due to the interference of tip operation by surface Ga atoms– the transfer of Ga atoms to the tip, have precluded the quantitative study of such a data.

If we check these images carefully, immediately apparent are the bright lines running along the [110] direction with a uniform spacing of 16Å in the [$\bar{1}$10] direction, corresponding to the four-times (4x) periodicity of the surface as observed previously by other groups [33, 61]. The high resolution image as discussed below reveals that along the [110] direction the surface has the 2x periodicity, thus the surface has the perfect 4x2 symmetry, as confirmed by our RHEED. It is interesting to note that there are only two types of defects observed on the 4x2 surface in comparison with the 2x4 phase. The first, most abundant one, is the complete Ga dimer vacancies from the 4x2 sub-unit which produce a depressed dark region separated by 8Å in the dimer-bonding direction. This type of defect becomes more noticeable in the immediate surroundings of the two-dimensional islands on the large terrace (Fig. 18(e)) and may well be important nucleation sites for growth. The second is the anti-phase boundaries due to the opposite phasing of the 4x2 sub-unit along the [110] direction, which is responsible for the transition from the 4x2 phase to the c(8x2) phase, as discussed below. They are associated closely with the first type of defects. Both types of the defects are similar to those appeared in the 2x4 surface [43]. It is interesting to note that a unique difference between these two surfaces is the complete absence of the so-called kinks where the 4x2 sub-unit shifts 4Å along the [$\bar{1}$10] direction, and shows no relationship with the increasing doping level in the present 4x2 phase. Thus the bright lines are running straightway through the entire terrace, demonstrating a high degree of ordering of the surface in the 2x direction. According to Pashley et al.[77], the kink density increases with increasing doping level and eventually forms a domain boundary in the case of the 2x4 As surface. Our experiments with the 4x2 surface having various doping levels do not support their claim.

Shown in Fig. 19 is a high resolution image of the 4x2 surface prepared by the UHV annealing process which exhibits more details than Fig. 17(e). It is our experience that this kind of high resolution image can never be obtained for the as-deposited defect-free surface (Fig. 17(e)). It is noted that each bright line in Fig. 17(e) and Fig. 18(e) is a doublet, consists of a pair of rows (yellow) separated by 5.1Å along the [$\bar{1}$10] direction, whereas the row itself is a chain of bright protrusions separated by 4Å along the [110] direction. A new finding here is faintly imaged features (blue) which are located in the outskirt of the paired row. The weak features (blue) always couple together to form a pair-like structure in parallel to the bright (yellow) rows. The separation between the neighboring pair-like features along the [110] direction was determined to be 8Å resulting in the 4x2 symmetry (a 4x2 unit cell has been outlined in the figure). The out-of phase arrangement of the 4x2 sub-unit gives rise to the c(8x2) symmetry.

We note that this image is basically the same as that obtained by Skala et al. [61]. However, our interpretation is completely different from theirs and supports a different model. We conjecture that the individual protrusions of the bright rows are the image of the *second layer* As atoms, not the Ga in the *first layer*, and that the pair-like faint features are indeed of the first layer Ga-dimers.

The only plausible model is the Ga-bilayer model proposed by Biegelsen et al. (Fig.3(b)). We have sample justifications for disproving the As-model in interpreting the present STM images:

(1) Our sample preparation process employed presently favors the Ga-rich surface. For successful growth of the as-deposited Ga-rich surface, the final exposure must be made with the Ga beam. The As/Ga flux ratio used is, thus, always lower than what needed for growing the 2x6 surface. Meanwhile, for preparing the annealed 4x2 surface, a temperature higher than that for the 2x6 surface is required, while the 2x6 surface is known to be more As rich than the 4x2 surface [33]. This observation is inconsistent with the As-model.

(2) The As-model cannot explain the measured height difference (only 0.6Å) between the bright row and the faint pair-like feature. For an ideal semiconductor surface, the As atoms have the doubly occupied dangling bonds and thus their STM image should be enhanced greatly in the filled states STM image, while the Ga atoms with the empty dangling bonds should be imaged faintly even if both the Ga and As atoms are located in the same surface layer. Thus, if the brighter protrusions correspond to the first layer As, a height difference of at least 1.4Å (1/2 H) (on basis of pure geometric consideration) is expected even without considering the strong As enhancement factor, contradicting with our observation of 0.6Å height difference. In reality because of this As enhancement, only the first layer As dimers should be imaged brightly without trace of the *second layer* Ga atom in the image, exactly the same way as the As imaging in the case of the As-terminated 2x4 surface [33,36,37,43,78].

(3) According to the As-model, the first layer As atoms form a dimer. A nodal structure or cocoon shaped feature should be expected for the filled states image. What we observed here, including those obtained by Skala et al., is quite different, showing just two isolated humps separated by 5.1Å unlike dimers.

(4) The As-model is in complete disagreement with the empty states image of the 4x2 surface, as shown in Fig. 19(b). Based on the out-of-phase arrangement of the humps along the [110] direction, we can assign each bright hump to be due to tunneling from the individual Ga-dimer. Thus, the As related features are completely absent from the image. If the surface consists of the

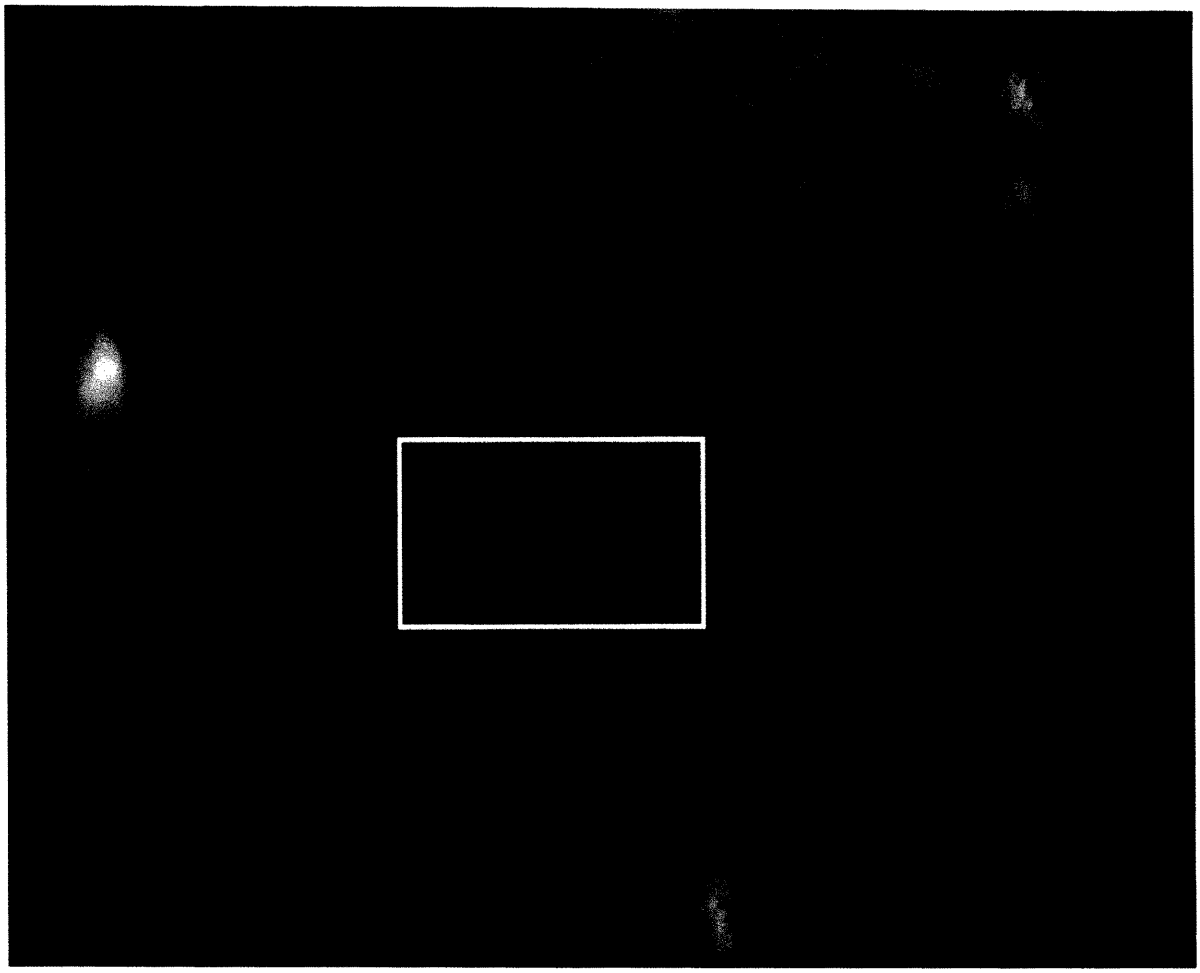

(a)

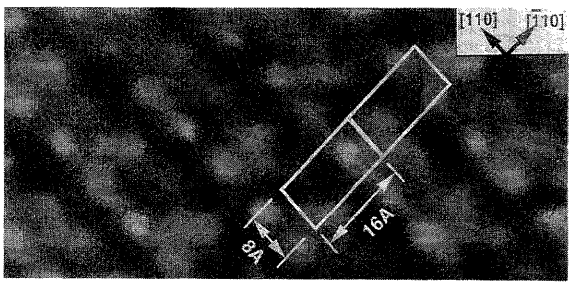

(b)

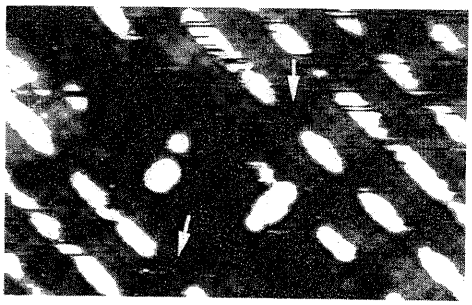

(c)

Figure 19. (a) Zoom-in filled states image showing the details of the 4x2 phase. The arrow indicates Ga cluster around which the Ga-dimers are imaged with enhanced brightness. The 4x2 unit cell is highlighted with a white rectangle. (b) Empty states image (at +2.2V) of the same surface as Fig. 19(a), showing the 4x2/c(8x2) symmetry clearly. A c(8x2) unit cell is indicated by the white rectangle. (c) High resolution filled states (at -2.2V) image of the GaAs(001)-4x2 surface with 0.5ML In, which renders additional support for the Ga bi-layer model. The arrows indicate the In-free regions where the image contrast changes.

first As-dimers according to the As-model, they should be clearly visible by the STM, similar to the situation occurred in the GaAs(001)-2x4 As surface where the empty states images show only the first layer As dimers [36,78].

In order to further demonstrate the brighter features being tunneling from the second layer As and the faint features coming from the first layer Ga, we have performed another set of experiments using the InAs/GaAs(001) heterostructure growth. Figure 19(c) is an STM image of the GaAs(001)-4x2 surface deposited with 0.5ML In. Comparing with Fig. 19(a), one can recognize beyond any doubt that the bright features in Fig. 19(a) are replaced by the In atoms and that faint paired features are imaged more brightly in Fig. 19(c). Particu-

larly in the regions where In is absent as indicated by the white arrows of Fig. 19(c), the bright features now become weaker than the neighboring paired features. Such an observation can never be explained by the As-model. This observation, further, renders additional support to our identification of the Ga-clusters, as discussed in Section 3.7. Therefore, the As model proposed by Skala et al. can be safely ruled out.

As for adopting the Biegelsen's Ga-bilayer model, however, there is an apparent problem between the model and the STM image; namely the pair-like faint features are located in between the protrusions forming the bright rows along the [$\bar{1}$10] direction, while the Ga and As atoms geometrically line up in the case of the Ga-model. This situation is more evident by a comparison of the Ga-bilayer model (the upper panel of Fig. 19(a)) and the segment of the image highlighted by white and black dots. Furthermore, the separation of bright rows is only 5.1Å much smaller than 8.0Å expected from the model. We believe that these are one of the main reasons for Skala et al. to discard it and to propose a new As-model (Fig. 3(c)).

As pointed out in Introduction, the overlapping first layer Ga and the second layer As orbitals are both accessible to the STM imaging in the range of applied negative bias voltage to the sample. Since the STM is probing the local density of states near the Fermi level, not merely the surface geometry, a correct interpretation of the STM image of this surface may not be so straightforward, compared with many other surfaces of semiconductors studied so far. In order to resolve these seeming discrepancies, we have performed a *first-principles total energy calculation of the surface charge density distribution based on the Ga-bilayer model.* The total energy was calculated within the local density functional approach. The total energy was minimized with respect to both the plane-wave coefficients of the occupied orbitals and the ionic degrees of freedom by using the conjugate- gradient technique. The details of the calculation methods have been described elsewhere [55].

The calculated results are shown in Fig. 20, which are the local density of the states from the 71st to the 76th bands at 0.9Å above the surface, based on the Ga-bilayer model structure. The 75th band is the HOMO (highest occupied molecular orbital)-derived band, which should be dominant in the filled state STM image. It has the charge localized at the second layer As (Peak B of the 75th band). As for the contribution by the top layer Ga-dimer to the filled state STM image, its charge distribution becomes noticeable only at the deep 71st HOMO-derived filled band. Furthermore, it peaks in the middle of the dimer (Peak C of the 71st band). It is evident that the charge distribution from the Ga-dimer gradually disappears with increasing energy levels (from 71st to 75th) and the As-derived charge becomes more dominant. As for the 76th LUMO (lowest unoccupied molecular orbital), its charge density is located at one of the dangling bond positions (Peak A) and should be basically empty for this ideal semiconducting surface.

Under the filled states STM imaging condition at -1.8V, we found that all local density of the states between the 71st and the 76th bands contribute to the tunneling current to form the STM image. Because of the smaller potential barrier height for tunneling from the 75th band, the 75th HOMO makes the most significant

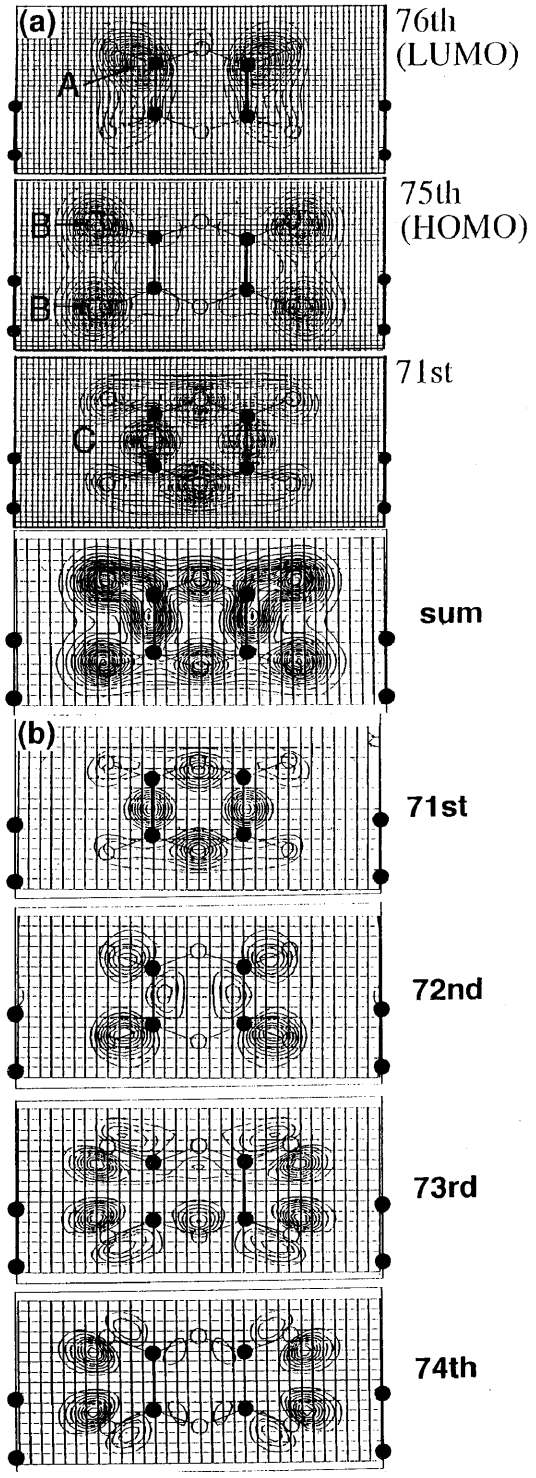

Figure 20. The charge distributions of the local density of the states calculated based on the Ga-bilayer model (Fig. 3(b)) at 0.9Å above the first layer Ga-dimer position for the 71st to 76th bands. The lowest panel displays a sum of the 71st, 72nd, 73rd, 74th and 75th bands.

contribution to the tunneling together with contributions from the overlapping 74th, 73rd and 72nd bands with the decreasing contribution, all of which are basically imaging of the second layer As atoms as individual brighter protrusions. On the other hand, the contribution for the top layer Ga dimer becomes only appreciable down at the 71st band at the middle of the Ga dimer. Thus, the top layer Ga dimer is observed as single faint hump (instead of pair-like feature) even though they are located in the top layer.

However, there are significant amounts of surface defects, such as adsorbates and vacancies which may be charge-accumulated, as indicated by the arrows in the image (Fig. 19(a)). As a result, the 76th LUMO-derived band is partially filled due to the charge transfer from the charge-rich singularities on the surface and contributes to the tunneling process. Therefore, we expect a nodal-like image for the Ga dimer.

The image of Fig. 19(a) basically corresponds to the total charge contribution shown at the bottom panel of Fig. 20, a sum of the bands from the 71st to 76th level. However, there is still some discrepancy between the STM image and our calculated charge distributions; that the maximum (A) of 76th LUMO is still too close to the maximum (C) of the 71st compared with the STM image (Fig. 19(a)) and thus the dimer looks somehow in between the two As along the [110] direction. It is found that the 76th LUMO orbital is drastically buckled and its charge center moves further away from the geometric center of the dimer with increasing distance from the surface, due to the influence of the third layer Ga dimers. Since the calculated density of states shown in Fig. 20 are the mapping by the charge distribution at only 0.9Å away from the surface while the STM image reflects the charge distribution at approximately 10Å away, Peaks A and B should further move away from the atom position.

Furthermore, the extent of the LUMO-derived band contribution to the filled states STM image depends on the amount of charge transfer to the Ga dimer dangling bonds. Taking all these effects into account, we could explain the STM image (Fig. 19(a)) and the Ga-bilayer model (Fig. 3(b)) self-consistently.

Unlike the As 2x4 surface where some three-dimer units were occasionally observed near defect sites, the STM images of the 4x2 surface prepared under various conditions all show the uniform two-dimer unit structure. Therefore, we conclude that there is no evidence to support a three-Ga-dimer model or a mixed As/Ga dimer model. In addition, our theoretical results show that both the three Ga-dimer model by Frankel et al. and the As-model by Skala et al. are energetically unstable compared with the Ga-bilayer model (Fig. 21) [79], in good agreement with the conclusion by Northrup and Froyen [56,57].

The successful observation of the as-deposited Ga-terminated 4x2 phase produced by MEE has a profound implication on the bilayer MBE growth mechanism of GaAs(001) surface (including all other III-V semiconductors). If the formation of the As-rich 2x4 structure is regarded as the first stage of growth cycle, it becomes

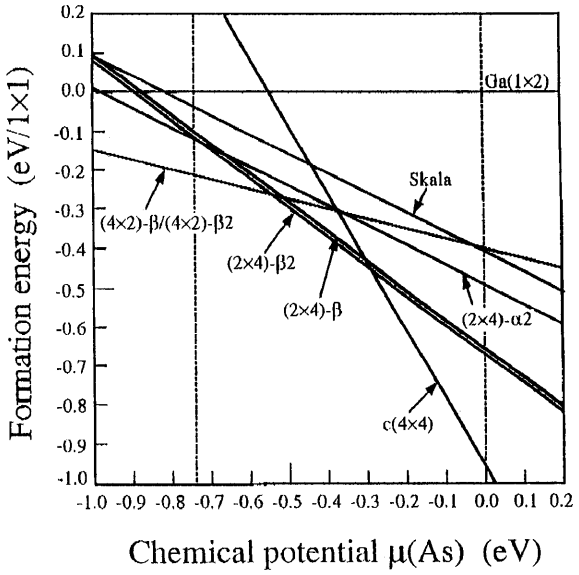

Figure 21. Surface formation energy for various GaAs(001) surface phases as a function of the As chemical potential. The energy is measured with respect to that of the GaAs(001)-Ga (2x1) surface. The As chemical potential is measured with respect to that of bulk As.

clear, by this direct observation, that when the impinging Ga atoms arrive at and adsorb onto the growing front at the second stage of growth cycle, the surface could be readily stabilized by the 4x2-Ga structure. We, therefore, speculate that the growth most likely proceeds by Ga/As coverage oscillation between the As-rich 2x4 and Ga-rich 4x2 reconstructions as one successively deposits alternative full monolayer of As and Ga, as documented in the atomistic process of the growth mechanism by Farrell et al. [14,17]. Switching of the specular beam intensity has never been observed experimentally under the normal MBE growth conditions, where the 2x4 RHEED pattern with somewhat diffuse background is continuously preserved throughout the growth cycle. This observation may be best understood in term of a so-called lock-in effect due to the rapid As chemisorption process (<0.1 s) on the Ga layer and extremely short residence lifetime ($<10^{-9}$ s) of Ga with respect to the scale of a growth cycle (growth of 1ML needs 1sec at the standard MBE growth rate of 1μm/hr) under the As supersaturation atmosphere [14,17]. Nevertheless, the present observation provides an experimental feasibility by which one may manipulate the growth stage precisely by varying the As/Ga flux ratio, thus we may be able to evaluate the actual growth process and control the growth conditions more accurately and effectively. Under this context, there is a logical optimism to reduce substantially the growth temperature and therefore improve the MBE performance.

In concluding this section, we wish to discuss an important implication of our conclusion together with our proposed scheme for As-rich 2x4 phase[43]. Figure 22 presents the ball-to-stick models of the As-rich 2x4 [43,54] and the Ga-rich 4x2 reconstructions. The sur-

face unit cell of the As-rich 2x4 phase has two As-dimers on the top layer and one As-dimer on the third layer (Chadi's two As-dimer model, [61], thus contains 3/4 ML of As on the surface, while the unit cell of the Ga-rich 4x2 phase has two Ga-dimers on the top layer and one Ga-dimer on the third layer and results in 3/4 ML of Ga on the surface. If one does not differentiate atom species, these two structures are just mirror-symmetric; either one can be obtained by 90° rotation of the other along the (001) crystal axis. Among all previously proposed models for the both surfaces, the surface charge neutrality can be maintained quite simply only for the present model scheme. Under this scheme, an addition of one ML of Ga atoms to the As-rich 2x4 phase results in the Ga-rich 4x2 phase and the addition of one ML of As on that surface simply transfers it to the original As-rich 2x4 phase, explaining readily switching between the 2x4-As and 4x2-Ga phases during our low temperature MEE process. Considering that the zinc-blend structure of GaAs and the polarization direction of the crystal is (001) direction, it is not difficult to understand this kind unified scheme.

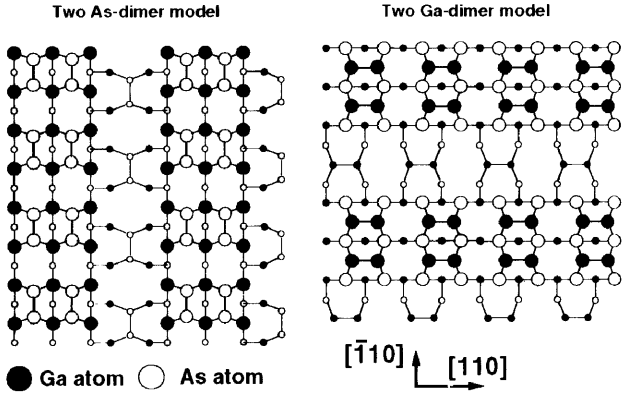

Figure 22. Atomic models for the GaAs(001) As-rich 2x4 (the left panel, see Ref. 53) and Ga-rich 4x2 (the right panel, see Ref. 33) reconstructions, demonstrating that two structures are essentially mirror-symmetric. Monolayer of Ga adsorption on the As-rich surface results in the Ga-rich 4x2 phase and monolayer of As deposition on the Ga-rich 4x2 phase turns into the As-rich 2x4 phase.

3.6. 2x6 reconstruction

We were able to prepare the 2x6 surface by both the MEE and the UHV annealing processes. The large scale STM images by these techniques are shown in Fig. 17(a) and Fig. 18(a). For preparing the as-deposited surface (Fig. 17(a)), an As/Ga flux ratio of approximately 10 with 2s alternative exposure was used, while the annealed surface (Fig. 18(a)) was obtained by heating the 2x4 surface at the temperatures at 550°C in UHV for around 15 min. These preparation processes reveal that this surface is less As-rich than the 2x4 phase but more As-rich than the 4x2 phase, and corresponds to a transition phase between the As-terminated and Ga-terminated phases. Both surfaces display a sharp 1x6 RHEED and LEED pattern with weak intermediate streaks [8,33]. This reconstruction has been investigated by Biegelsen et al. by using STM [33] and by Qi et al. in the polarized infrared spectra study recently [80]. According to Biegelsen et al.'s notation, the 2x6 and 1x6 are basically the same structures, we will not distinguish them in the present study. The proposed atomic model by Biegelsen et al. which we basically agree with is shown in Fig. 3(d) [81].

It is found that the ball-and-stick model shown in Fig. 3(d) only reflects the ideal case. The top layer As dimers are not always arranged with perfect order in zigzag shape along the 2x direction, as revealed in the close-up image from the annealed surface (Fig. 23(a)). Furthermore, the weak features between the bright rows appear to have 4x (not the 2x as shown in the model) periodicity which was assigned as the image of the second layer Ga atoms [33]. This situation is also observed in the image of the as-deposited surface (Fig. 23(b)). In this high resolution image, we are able to resolve the faint features between the bright rows which possess the 4x symmetry along the [$\bar{1}$10] direction and are arranged into the dimer-building-block configuration, the totally same manner as that in the pure 4x2 surface.

We have also obtained the dual bias voltage images from the as-deposited surface, which are shown in Fig. 23(c). The left panel corresponds to the filled states image while the right panel corresponds to the empty states one. The regularly separated humps in the empty states image clearly exhibit its characteristic 4x periodicity mentioned above. Comparing these dual images, the empty states image (the right panel) obviously shows somewhat higher contrast for the weak features between the brighter rows in the filled states image. As for the GaAs(110) surface [70], we expect the filled states to be concentrated on the As atoms and the empty states to be concentrated on the Ga dimers. Our observation that the enhanced contrast in the empty states image is restricted to the weak features between the rows is, therefore, consistent with the assignment that the top layer surface atoms are As and the second layer atoms exposed between the rows are Ga, as suggested in the model (Fig. 3(d)). In the central part of line A (indicated by the arrow) where a narrow As island is capped with another layer Ga (most likely five dimer-building-blocks, as discussed below), the dual bias voltage images show the reversed contrast for the central part and both ends of the line. Thus, if As/Ga exchange occurs as reported by Falta et al.[31], it should be readily observed by STM dual imaging. In addition, this observation also disproves the idea that the 2x6 is more Ga-rich than the 4x2 phase [31].

It is interesting to note that we could image the empty states Ga dimers clearly in the case of the 2x6 phase, which was very difficult in the case of the pure 4x2 surface. Since electrons tunnel from the Ga empty orbitals in the right panel of Fig. 23(c), one would expect to observe a nodal structure for the Ga-dimer. However, Ga-

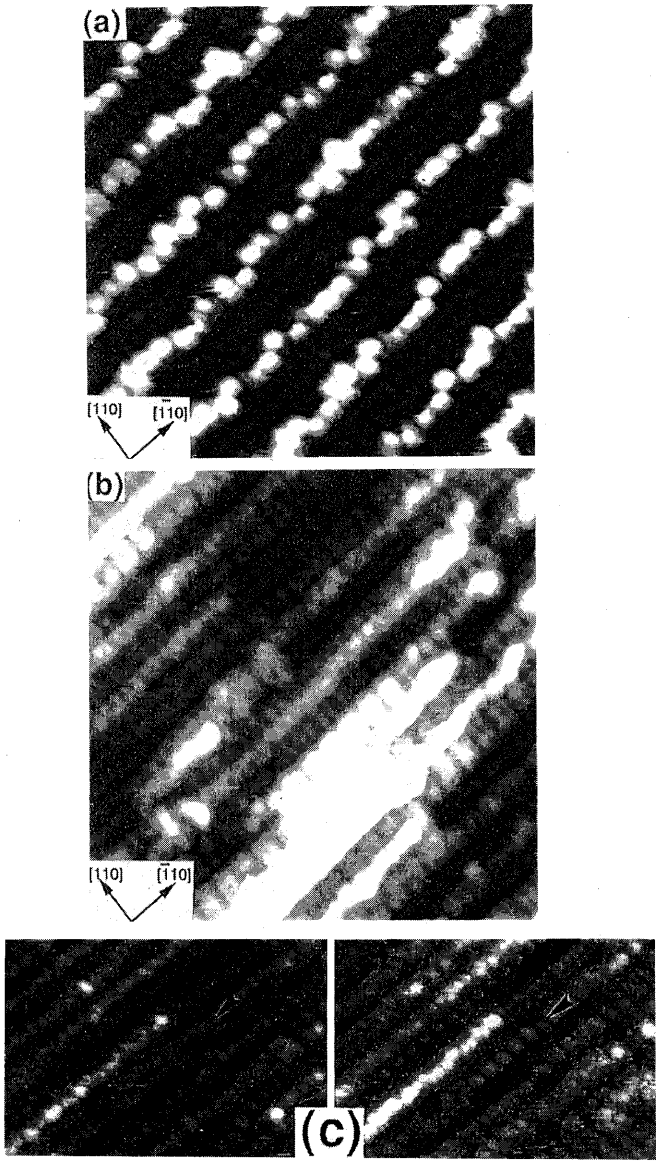

Figure 23. The filled states STM images obtained for (a) (130Å×130Å) annealed and (b) (230Å×230Å) as-deposited 2x6 phase. (c) The dual bias voltage images from the as-deposited 2x6 phase. The left panel corresponds to the filled states (at -2.5V) and the right panel the empty states (at +2.5V).

dimer was imaged as an individual hump, which apparently results from the electronic effect. Our images are, unfortunately, not of sufficient resolution to determine the details, and unambiguous identification of these features needs an in-depth theoretical consideration of the electronic properties. This complication precludes us to discuss further at this moment on the atomic structures over the above model. In any case, any plausible model must include the As-As dimer and Ga-Ga dimer building blocks as shown in the model (Fig. 3(d)), together with a consideration of the 4x periodicity for the Ga-dimer ordering. It may be fair to regard this surface as a transient phase since it doesn't have a complete ordering, as indicated by Biegelsen et al.[33].

3.7. "Genuine" 4x6 reconstruction

We have identified two distinctly different 4x6 phases by direct STM observations. We first discuss the one which exhibits the "genuine" 4x6 translational symmetry. If we annealed the 2x6 surface in vacuum at 600°C for more than 20 min or deposited further at 500°C using the higher Ga flux ($As_4/Ga = 6$) than that needed for the 4x2 phase in the MEE on the 2x6 surface, a more Ga-rich "genuine" 4x6 phase was observed by STM, whose symmetry being confirmed by RHEED. Large scale images from the annealed and as-deposited surfaces are respectively shown in Fig. 17(g) and Fig. 18(g). In Fig. 17(h), we show a typical close-up image of this "genuine" 4x6 reconstruction. In their STM study of the GaAs(001) Ga-rich surface reconstructions, Biegelsen et al. reported that they had obtained the surface which has a true 4x6 symmetry using the annealing process similar to ours. We, thus, believe that our STM data and theirs are an identical 4x6 phase.

The "genuine" 4x6 phase is uniquely characterized by the regular array of large oval protrusions located at each corner of the unit cell. These oval protrusions always occupy the middle of the As rows of the 4x2 surface. By superimposing the 4x2 phase model with the 4x6 phase image, the 4x periodicity of the surface in the [$\bar{1}$10] direction becomes immediately evident. The separation between the protrusions along the [110] direction is measured to be 24Å thus, clearly demonstrates the 4x6 symmetry of the surface. If the surface was scanned with improved tip conditions, much higher resolution images could be obtained. One of the examples is shown in Fig. 24. In this atomically resolved filled states image, the individual Ga atoms forming a dimer with enhanced contrast are clearly resolved. The 6x periodicity is more easily identified by the regular array of the large oval protrusions in every three Ga-dimers along the [110] direction. We also observe how the presence of the Ga-dimer vacancy defect (indicated by the white arrow) causes the c(8x2) symmetry by a 4Å shift of the 4x2 sub-unit along the [110] direction.

The oval features are ~1.0Å (~1/2 H) higher than the Ga dimers but are lower than the 2x6 As rows by 0.9Å. Their spatial distribution extends approximately 3-4 a0 (a0=4Å is the surface lattice constant) in the [110] direction and ~2 a0 in the [$\bar{1}$10] direction. We speculate that such high contrast imaging of the Ga dimers is clear indication of significant charge transfer from the oval protrusions to the charge-depleted Ga dimers. We have documented in Section 3.5 that the atomically resolved image cannot be obtained on the completely defect-free 4x2 surface (where this type of features is completely absent). This is exactly what is observed in the STM image of the as-deposited 4x2 surface (Fig. 17(e)), where only the As-derived features are imaged with no Ga-derived feature at all.

The origin of this contrast enhancement effect is demonstrated more markedly when a single oval protrusion adsorbs on the pristine 4x2 surface, as indicated by the arrow in Fig. 19(a). In the immediate surrounding regions of the oval feature (in yellow), the Ga dimers

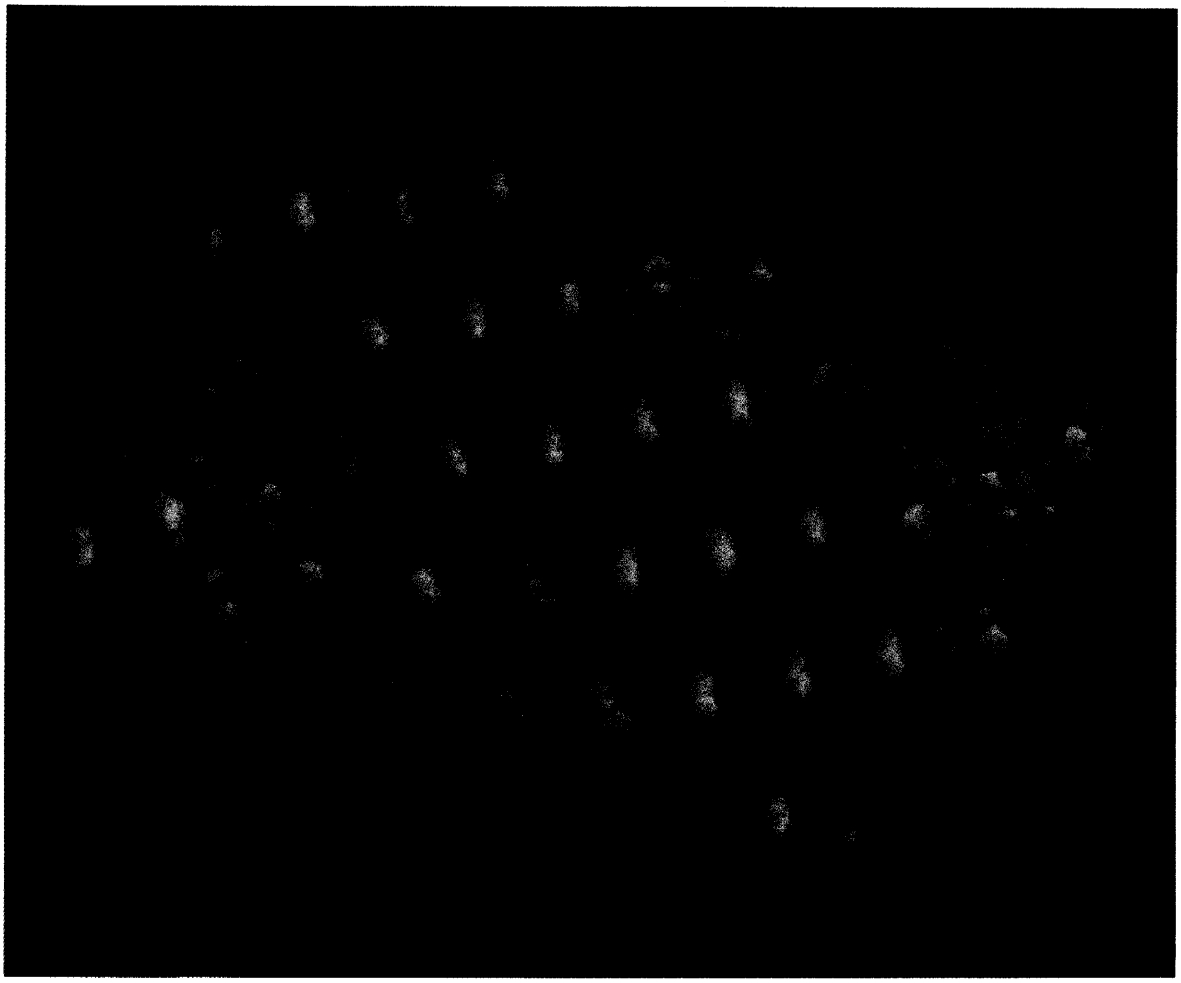

Figure 24. Three-dimentionaly displayed genuine 4x6 STM image.

become suddenly brighter and the As rows become faded out. With increase in the number of the oval shape features, the image contrast between the As and Ga atoms of the 4x2 surface shifts and eventually reverses completely, resulting in that of the 4x6 surface (Fig. 25).

Fig. 25 is the gary-scale 4x6 STM image. The line scan taken on the top of the Ga-dimers along the [110] direction, which further justifies the present argument. The brightness asymmetry of individual dimers is evident in the line scan, which is attributed to be charge screening effect of the large oval feature. The closer the distance of the dimer and the oval feature is, the greater the degree of the asymmetry is. The dimer surrounded by several oval protrusions looks somewhat symmetric, due to equal degree of charge transfer.

The identification of these large oval features located at each corner of the 4x6 unit cell has been successfully carried out by another set of experiments which will be discussed in detail in Section 3.9 [66]. Together with the heavily Ga-rich sample preparation processes, we have conclusively determined that they are Ga-rich clusters. Based on the observation of the evolution of these oval features, we propose a first atomic model for the "genuine" 4x6 surface, which is also shown schematically in Fig. 25 in the same scale as the experimental STM image. According to this model, the 4x6 phase is the Ga-rich 4x2 phase with extra Ga clusters orderly distributing on the surface. Since the cluster usually exhibits different electronic properties compared with the corresponding bulk bonding material, it should be of great interest to determine the detailed nature of these clusters. The scanning tunneling spectroscopy investigation is underway currently. Considering the measured height difference of the Ga cluster and dimer (1.0Å), we speculate that these clusters are flat and two-dimensional and consist of 6-8 atoms depending on their growth process.

An interesting observation is that these large oval protrusions occasionally disappear and are imaged as a dark dumbbell-shaped structure at small bias voltages as seen in Fig. 25(a),(b). A simple explanation is the transfer of Ga atoms from the surface to the tip. But the bias

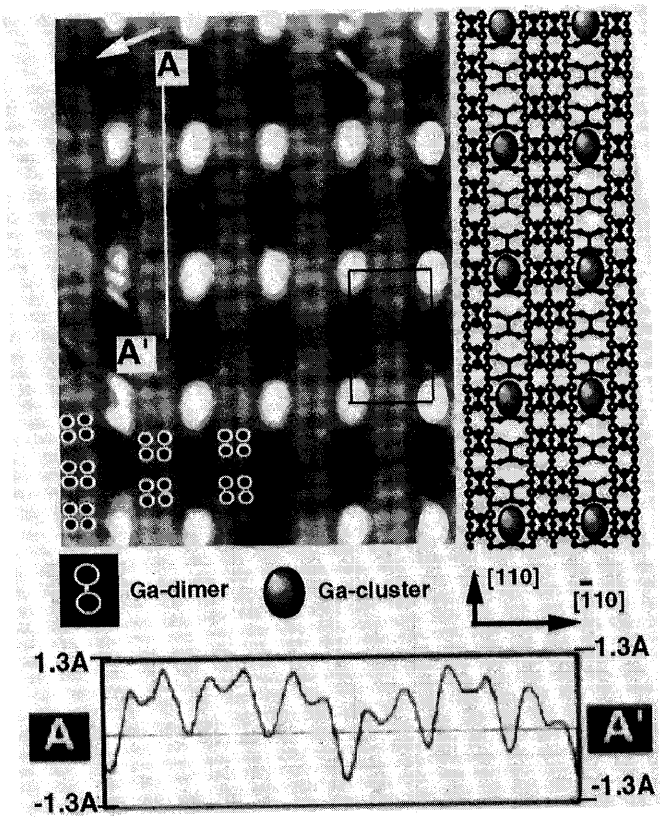

Figure 25. Atomic resolution filled states STM image of the "genuine" 4x6 surface taken at -1.8V(upper panel). In this image, individual top-layer Ga atoms forming a dimer can be clearly resolved, as highlighted by the white open circles. The line plot (from A to A' in the STM image) is shown in the lower panel. The height asymmetry within the dimers is clearly visible, which is due to the charge transfer from the Ga-clusters. The 4x6 unit cell is indicated by a black rectangle. The white arrow in the upper left indicates a missing-atom defect, which causes the transition between the out-of-phase and the in-phase arrangements of the 4x2 sub-unit. The schematic shown in the right side of the STM image is the atomic model proposed in this study.

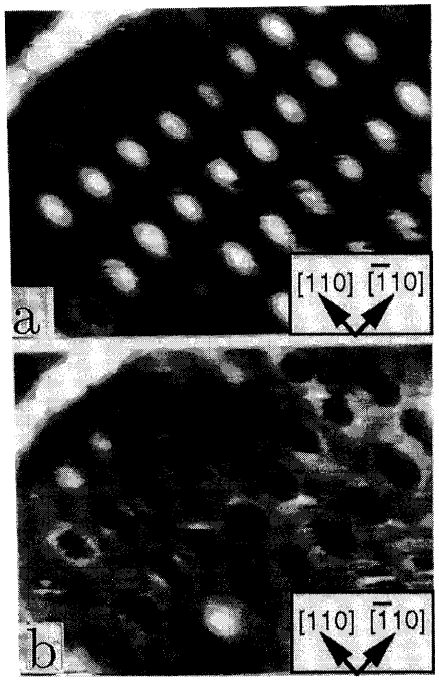

Figure 26. (a) and (b) (100Å×90Å) show the voltage-dependence of the oval image of the clusters. The dumbbell shape clusters are evident in (b). Images are tunneling from the filled states, but with different bias voltages: (a): -2.0V and (b): -1.6V.

voltage-dependence images show that this is not the case and that it must result from electronic effect in tunneling: the observation of the dumbbell structure is not related to the tip conditions and appears at only relatively small bias voltages, 0 >Vb >-1.6V. As we discuss it later in detail, these oval protrusions are identified to be the Ga-clusters. The Ga-cluster has been believed to be semiconducting, and due to the weaker bonding among the atoms and decreased atomic number in comparison with the bulk material, the energy gap (Eg) becomes wider and the local density of the states should significantly decrease near the Fermi level which is accessible to the STM. Considering this modified electronic structure of the Ga cluster, the local density of states near the Fermi level is reduced significantly and stable tunneling cannot be maintained. Thus, when the surface is scanned along the horizontal direction and the tip encounters the cluster, the imaging process may suddenly experience a marked decrease in tunneling current, and then recovers to the normal case once the tip passes the cluster. Higher noise level one can see in the cluster region (Fig. 25(b) is consistent with this mechanism. A similar phenomenon was observed in the cross-section STM images of AlGaAs/GaAs by Salemink et al.[82].

3.8. "Pseudo" 4x6 reconstruction

It has been surmised, based on the LEED study [8], that the 4x6 diffraction pattern most likely results from the co-existence of the nx6 and 4x1 reconstructed domains rather than the single phase of 4x6 symmetry. Now we discuss the second 4x6 phase which displays basically the identical RHEED diffraction pattern to the "genuine" 4x6 surface discussed in the previous section (3.7) but is completely different from it on the atomic scale structure. Typical examples are shown in Figs. 27(a) and (b). The surface for Figs. 27(a) was prepared by annealing the 2x6 phase at 600°C for 5 min. In Fig. 27(a), there is an intermediate-size island (150Å ×150Å) in the center of a large flat terrace of the 4x6 phase. The island was measured to be 2.8Å higher than the terrace. The unique zigzag rows in the [$\bar{1}$10] direction represent the remaining 2x6 reconstruction during the As desorption by the high temperature UHV annealing. As for the large bright features on the terrace and the island, they form the "genuine" 4x6 symmetry as discussed above. The height profile (a–b) is shown in the lower panel of the image. The solid reference lines are for the 2x6-As

feature and the dotted reference lines are for the Ga-clusters. The measurement is calibrated by the known height of the GaAs(001) bilayer step (2.8Å). The cross-section analysis clearly reveals that the Ga-cluster is approximately 0.9Å lower than the 2x6-As feature when they are located in the same layer. Therefore, the image demonstrates a coexistence of the 2x6 phase and the "genuine" 4x6 phase. In Fig. 17(f) and Figs. 18(f), (g), we can observe how the As 2x6 phase gradually disappears and the "genuine" 4x6 evolves at the same time, with the increasing annealing temperature and/or longer annealing time or higher Ga flux in the MEE cycle. Another interesting finding is that the As 2x6 phase is always located or nucleates near the step edge or surface defects. Figure 27(a) shows how the formation of the 4x6 phase closely links to the As desorption of the 2x6 phase on the terrace: namely, the 2x6 phase transforms so readily to the "genuine" 4x6. This is the reason why the 4x2 surface cannot be easily prepared by the annealing process or the MEE deposition.

Shown in Fig. 27(b) is another case: coexistence of the 2x6 phase (characterized by the zigzag lines along the [$\bar{1}$10] direction) and the 4x2 phase (characterized by the doublet lines along the [110] direction). This is exactly what is expected by the LEED studies [8, 74]. As shown in the panel below the STM image, the cross-section profile (c–d) indicates a height difference of approximately 1.4Å between the 2x6-As and the 4x2-Ga related features. We can prepare this kind of surfaces by either annealing or MEE by setting an appropriate Ga/As flux ratio. By increasing the Ga coverage with increasing temperature and extended annealing time or higher Ga flux during MEE, the 4x2 domain becomes more and more abundant than the 2x6 domain on the surface and vice versa, as evident in Figs. 17(b), (c) and (d) and Fig. 18(d). These preparation processes further point out that the As surface composition of the 2x6 phase must be higher than that for the 4x2 phase.

We also note that a new irregular structure formed in the annealed surface which dominates in Fig. 18(d), coexisting with the 4x2 phase. The new structure seems to have no long-range ordering with the exception in the region near the 4x2 domain. We therefore call it as a "disordered phase". We believe that this disordered phase is a Ga-rich phase, based on the following observations:

(1) the surface preparation process suggests that it should be more Ga-rich than the 2x6 surface. According to the Biegelsen et al.'s model [33] which we concur (see Section 3.6), the As coverage of the 2x6 surface is 1/3 ML. For preparing the structureless surface by UHV annealing (evolution seen in Fig. 18), we must use a higher temperature than that needed for the 2x6 phase (Fig. 18(a) → (b) → (c)). Further annealing results in the coexistence of the structureless and Ga-rich 4x2 surface (Fig. 18(d)), and then uniform formation of the Ga-rich 4x2 pristine surface (Fig. 18(e)). It is known that annealing of the GaAs(001) surface results in As desorption from the surface and thus increase in the Ga coverage. Therefore, the surface coverage of the structureless region should be between that of the 2x6 phase (2/3ML-Ga (=1/3ML-As)) and that of the Ga-rich 4x2 (3/4ML-Ga). (2) We have successfully obtained the images under both positive and negative sample bias and comparison between the filled state and empty state images supports the Ga-rich nature of the surface. Figures 28(a) and (b) show the filled and empty states images of the co-existing 2x6 and structureless surface, respectively. The height- profiles at the location indicated by the black lines in images are shown in the panels below the STM images. The measurements yield 1.6±0.32Å in the case of the filled states image and 1.1±0.15Å in the case of the empty statesas for the height difference between the 2x6 As feature and the disordered features. This indicates that the contrast between the features for the 2x6 and disordered regions for the empty state image (Fig. 28(b)) is smaller than that for the filled state

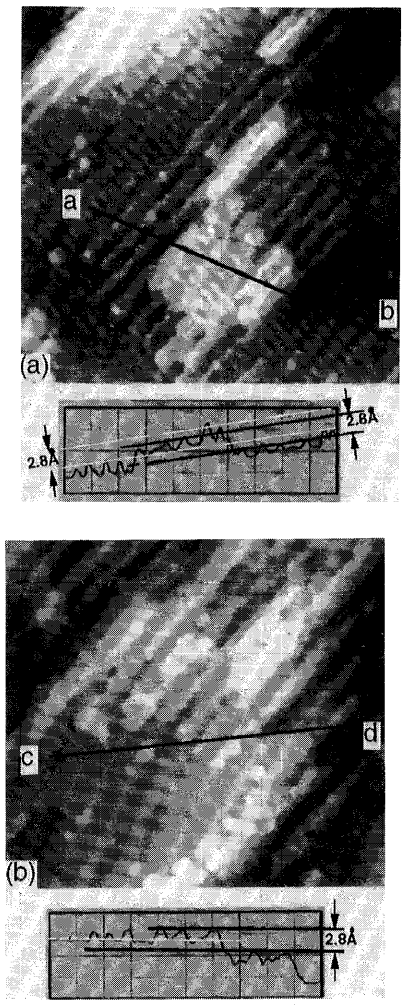

Figure 27. The filled states STM images of (a) (440×290Å) the mixed 2x6+"genuine" 4x6 phases, and (b) (420×270Å) the mixed 2x6+4x2 surfaces. The cross-section profiles (a—b in (a) and c—d in (b)) are shown right below the corresponding images. Both surfaces display the similar 4x6 RHEED pattern.

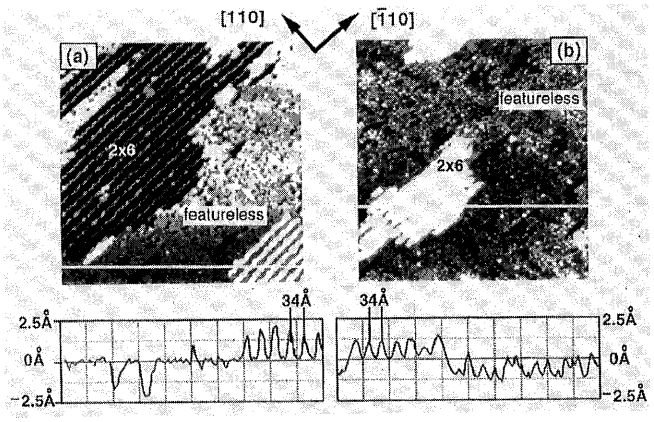

Figure 28. Typical filled and empty states STM images (750Å×750Å) of the co-existing 2x6 and disordered surface at negative (-2.0V) and positive (+2.0V) sample bias, respectively. The line plot depicted by the white line in the image is shown in the corresponding lower panel of the image. Two images were taken from different regions of the same surface. Note that the contrast change between the features for the disordered and the 2x6 regions.

image (Fig. 28(a)) by 0.5Å namely, the contrast for the disordered feature is enhanced in the empty states image. Since the filled (empty) states STM images are preferentially concentrated on group V-As (III-Ga) sites [70], the observed contrast change from Fig. 28(a) to Fig. 28(b) with bias variation leads us to conclude that the disordered phase be related the Ga atoms.

We note that this disordered structure was never observed from the as-deposited surface by MEE. Also it was never observed as a single phase. In Figs. 18(c) and (d), we see the development of this structure upon the As depletion during the continuous annealing. At higher temperatures, they will disappear and transform into the 4x2 phase or the "genuine" 4x6 phase. Since the annealing temperature where this phase stabilizes is not high enough for the formation of the 4x2 phase, it is appropriate to regard it as a transient phase before the 4x2 phase.

Concluding this section, we wish to point out an important fact that the "pseudo" 4x6 reconstruction can be indeed divided into two cases: the first one is a coexistence of the 2x6 and the 4x2 phases with/without a structureless Ga-rich phase, and the second one is a mixture of the 2x6 and the "genuine" 4x6 phases. Because of these mixed phase characteristics, the surface composition observed by AES and XPS can vary in a wide range. Without careful analysis on truly an atomic scale using the STM, the 4x6 phase can never be understood precisely.

3.9. New 4x1 phase

In this section, we briefly discuss a new structure-the 4x1 surface (Fig. 18(h)). The basic characteristics of this newly defined 4x1 phase are the same as that of the "genuine" 4x6 surface. They consist of the Ga 4x2 structure as a sub-unit, which is modulated with randomly distributed oval-shaped Ga clusters along the [110] direction, as shown in the close-up image (Fig. 29). The RHEED pattern for this surface displays a sharp 4x1 symmetry. We, therefore, call this phase as the 4x1 reconstruction. This surface was prepared with higher annealing temperatures (at 650°C for 10 min) than those for the "genuine" 4x6 surface. In this image, the faint stripes running along the [110] direction are the image of the second layer As lone pairs, characteristic of the 4x2 structure. Also observed in the image are several larger circular protrusions (indicated by arrows). We identify that they are the larger Ga clusters consisting of more Ga atoms since the desorption of As from the surface becomes more drastic due to the higher temperature annealing. In the large area image (Fig. 18(h)), we see even larger features; Ga droplets as indicated by arrows. As for the Ga-clusters, their density in the 4x1 surface is measured 15% higher than the ideal 4x6 phase (Fig. 25) and it increases with further annealing time. To our knowledge, the 4x1 phase is the most Ga-rich phase among various structures reported so far. Even though these Ga clusters are uniformly separated by 16Å along the [$\bar{1}$10] direction, the distribution along the row ([110] direction) is less ordered, forming a meandering long worm-like feature. Together with the genuine 4x6 phase where the Ga-rich clusters are arranged in a perfect fashion, it is speculated that there exists a strong attractive interaction between the neighboring Ga clusters; the separation of 16Å does not shield its interaction completely while 24Å is long enough to decay. Further annealing (for example at 700°C) causes the decomposition of the material and extremely rough morphology, and no ordering was observed unlike the case of the InSb(001) surface which exhibits a 1x1 symmetry under the similar annealing [83]. This structure might be the last stable single phase under the static

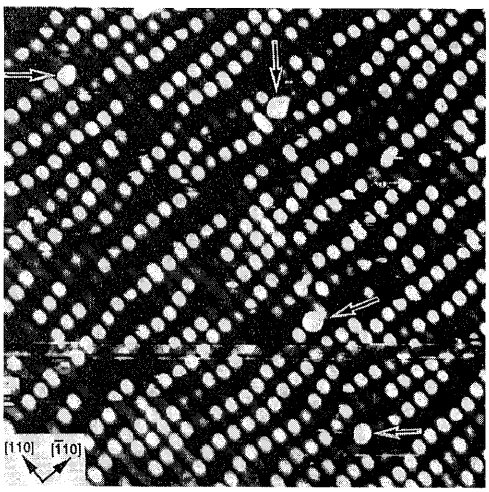

Figure 29. The close-up filled states STM image (490Å×490Å) of the newly defined 4x1 phase. The arrows indicates four larger Ga clusters (Ga droplet precursors) compared with the regular size ones.

Ga-rich condition for the GaAs (001) surface.

3.10. Surface composition

Extensive efforts have been rendered to determine the surface compositions of the Ga-rich surfaces by different techniques [7-9,12, 20, 64, 74]. The main results obtained by those studies for the 2x6, 4x2 and 4x6 surfaces are summarized in Table I. Because of different characterization techniques being used, it is not possible to compare the absolute surface composition with the single standard. While basically consistent results are obtained in the case of the 2x6 surface with an exception [8] which claims that the 2x6 is more Ga-rich than the 4x2 phase, there is a serious discrepancy in the relative composition for the 4x6 and 4x2 surfaces [7-9,12,20,64]. Although most studies reported less Ga-rich nature of the 4x2 surface with respect to the 4x6 phase [8,12,20], Bachrach et al. suggested that the 4x2 surface is As-rich than the 4x6 surface by 0.2ML, and Creighton concluded that the composition is the same for the 2x6 , 4x2 and 4x6 surfaces [64].

reconstruction	4x6	4x2	2x6
Ref. 5 (Auger As/Ga)	x	2.0	2.5
Ref. 6 (Auger As/Ga) θ_{As}	0.27ML	0.22ML	0.52ML
Ref. 9 (core-level 3d As/Ga) θ_{As}	0.33ML	0.52ML	0.42ML
Ref. 10 (core-level 3d As/Ga)	0.91	0.78	x
Ref. 16 (Auger As/Ga)	1.27	1.27	1.27
Ref. 22 (average As coverage) θ_{As}	0.54ML	0.09ML	x
Ref. 21 (core-level 3d As/Ga)	overlap with the 4x2	0.8--1.0	x

Table 1. Summary of surface Ga/As composition vs. various GaAs(001) surface phases reported by previous workers.

As discussed in Sections 3-7 & 8, the 4x6 surface is not necessarily a single phase. It can be either (1) mixture of the 2x6 and 4x2 phases, or (2) mixture of the 2x6 and the "genuine" 4x6 phases, or (3) the single "genuine" 4x6 phase. Which domain appears and how large the size of a given domain is in the course of the phase transition depend critically on the preparation process. Since these local variations cannot be detected by the standard analysis techniques, such as AES, any claim of the composition will be ambiguous and highly speculative.

According to the structural models discussed in Sections 3-5, 6, 7, 8 and 9, the 2x6 surface is most As-rich and the "genuine" 4x6 surface is most Ga-rich while the 4x2 surface has an intermediate surface composition with a well-defined narrow range. When the "pseudo" 4x6 is a mixture of the 2x6 and 4x2 phase, it should always be As-rich than the 4x2 phase, as reported by most studies [6,7]. It finally reaches the composition value of the 4x2 surface with the increasing annealing temperature or higher MEE Ga flux [64]. On the other hand, when the "pseudo" 4x6 is formed with the 2x6 and "genuine" 4x6 phases, the situation is rather complicated. The surface composition can be either As-rich (the 2x6 phase dominates on the surface) [8,12,20,74], or Ga-rich (when the "genuine" 4x6 dominates on the surface) [9], or the same as that of the single phase 4x2 structure (when the 2x6 and "genuine" 4x6 phases mix with an appropriate domain ratio [64] and thus overlaps with that for the 4x2 surface [74]).

In the decomposition region, the "genuine" 4x6 phase dominates on the surface, and the composition is always Ga-rich. Under this scheme, the surface composition with the 4x6 diffraction symmetry can vary from 0.33ML As in the extremely As-rich side to more than 1ML Ga in the extremely Ga-rich side (for the 4x1 surface).

Because the parameters used to define the sample preparation are different from one group to another, the accurate comparison between the present data and all others is not easy. Nevertheless, we can, under this scheme, consistently explain almost all previous observations. We believe that we have overcome the major hurdle in understanding the atomic structures and that we were able to determine the surface compositions of various phases.

We summarize our results with a schematic evolution diagram shown in Fig. 30, where various phases are plotted as a function of As/Ga surface coverage. Three different coverages: 0.3ML-As, 0.75ML-Ga, and approximately 1ML-Ga are noted along the horizontal axis, corresponding to the 2x6, 4x2, and "genuine" 4x6 (G4x6) phases, respectively. All the phases being discussed in the present work are placed according to their surface compositions. The lower path is the evolution of the surface phase during the MEE growth with increasing Ga flux and the upper path is that due to annealing with increasing temperature. The "pseudo" 4x6 (P4x6) phase indeed has a variety of surface composition, its value stretches from 0.33 ML As (for the 2x6 phase) to 1ML (for the G4x6 phase). According to this diagram, with the increasing Ga concentration, the 2x6 phase undergoes a transition from the 2x6 + 4x2 mixed structure to the G4x6 phase via the 2x6 + G4x6 mixture. After that, the surface usually transforms into the Ga-rich 4x1 surface. In the case of annealing, the disordered Ga-rich phase (D) always exists. This disordered phase may play an important role in the continuous evolution. The evolution may also take place with a different transition path: the 2x6 phase may directly change into the 4x2 phase under certain conditions, for example deposition of right amount of Ga density by MEE should produce the perfectly flat 4x2 surface without any 2x6 island. This transition is found to be irreversible.

As for the co-existence of various phases, Yamaguchi and Horikoshi have recently studied the transition between the 2x4 As and 4x2 Ga phases by STM, RHEED specular intensity measurement and Monte Carlo simulations [44]. They have found that the transition be-

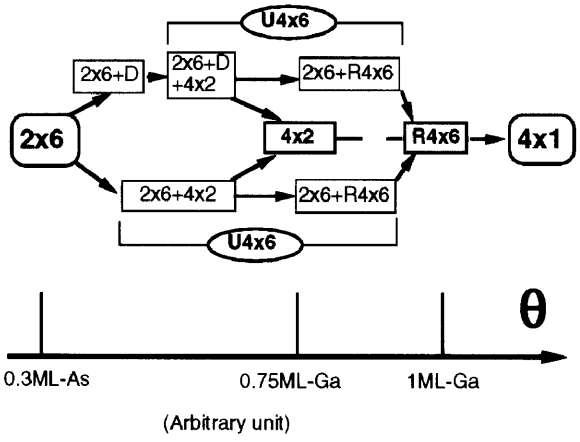

Figure 30. The phase evolution diagram of the GaAs(001) Ga-rich surface as a function of Ga coverage. In the figure, D represents the disordered (structureless) region in Fig.18 (b), (c) and (d). P4x6 represents the "pseudo" 4x6 phase and the G4x6 the "genuine" 4x6 phase.

tween the 2x4 As and the disordered 3x1 phases is second-order while it is the first-order nature but continuous in the case of the Ga-rich regime (3x1 $\rightarrow$ 4x2) due to finite size effects. Therefore, the present observation of the stable, mixed Ga-rich domains (2x6 + D, 2x6 + D + 4x2 + "genuine" 4x6) between the 2x6 phase and the 4x6 phase is consistent with their conclusion.

4. Conclusions

Atomically resolved STM, RHEED, RHEED intensity dynamical analysis and first-principles total energy calculation have been carried out in order to systematically investigate various GaAs(001) surface reconstructions and the following conclusions are obtained[86]:

1). The unit cell of the α, β and γ phases all consist of the two As dimers and two dimer vacancies and the α and β phases have different second and third layer structures.

2). The α phase is the two-As dimer model proposed by Farrell and Palmstrom with relaxation incorporated by Northrup and Froyen, the surface coverage of the α phase is 0.5ML of As; The β phase is the two-As-dimer model proposed by the Chadi, the surface coverage of the β phase is 0.75ML of As. The γ phase is the mixture of the β phase and the c(4x4) phase with surface As coverage varying between 1.75ML and 0.75ML depending on the growth conditions.

3). The atomic structure of the 4x2/c(8x2) reconstruction can be described best by the Ga-bilayer model proposed by Biegelsen et al. It is found that this surface has a well-defined surface composition of 0.75 ML Ga. The seeming discrepancy between the atom-resolved high resolution STM image and the Ga-bilayer model was finally resolved based on our analysis utilizing a first principles total energy theory and its calculated surface charge density distribution.

4). Our unified scheme for the GaAs(001) surface; two Ga-dimers at the top layer and additional Ga-dimer at the third layer for the Ga-rich 4x2 phase and two As-dimers at the top layer and additional As-dimer at the third layer for the As-rich 2x4 phase, a mirror image in atomic structure, may be the key for the smooth layer-by-layer GaAs(001) growth by MBE.

5). We have documented, without any ambiguity, that there are two different 4x6 diffraction symmetry phases by direct observations of a phase transition in the Ga-rich regime reconstructions. One of them is the more Ga-rich single phase (we call it as "genuine" 4x6 phase) and the other is the less Ga-rich mixed phase ("pseudo" 4x6 phase) in reference to the 4x2 phase. The evolution path was determined among the 2x6, P4x6 and G4x6 phases.

6). The "genuine" single 4x6 phase, which is characterized by the perfect array of large Ga- clusters located at every corner of the 4x6 unit superimposed with the 4x2 Ga-bilayer structure. This is the first atomic model ever proposed for the "genuine" 4x6 phase. With additional Ga deposition, the "genuine" 4x6 phase transforms into a newly defined 4x1 symmetry phase, which is characterized by increased number of the Ga-cluster randomly distributed along the [110] direction on the 4x2 surface.

7). The "pseudo" 4x6 phase is merely a mixture of various phase. Actually, it can be further divided into two different configurations: one is the coexistence of the reconstructed 2x6 and 4x2 domains and/or a disordered Ga-rich domain, and the other is the mixed 2x6 and "genuine" 4x6 domains. The former is always As-rich compared with the 4x2 surface, whereas the latter results in a wider composition range, which varies from more As-rich to Ga-rich and overlaps with the 4x2 reconstruction.

Acknowledgements

The project was partially supported by Grant-in-Aid for Scientific Research of Ministry of Education (Nishina Project: 05NP0501) and by Grant-in-Aid for Scientific Research, Specially Promoted Research (Project number: 08102001), Ministry of Education, Japan.

1) F. Jona, IBM Res. Develop. 9, (1965) 375.
2) A. Y. Cho, J. Appl. Phys. 42, (1971) 2074.
3) A. Y. Cho, J. Appl. Phys. 47, (1971) 2841.
4) J. R. Arthur, Surf. Sci. 43, (1974) 449.
5) A. Y. Cho and J. R. Arthur, Prog. Solid State Chem. 10, (1975) 157.
6) J. H. Neave and B. A. Joyce, J. Cryst. Growth 44, (1978) 387.
7) A. J. Van Bommel and J. E. Crombeen, Surf. Sci. 57, (1976) 437; A. J. van Bommel, J. E. Chrombeen and T. G. Van Dirschot, ibid 72, (1978) 95.

8) P. Drathen, W. Ranke, and K. Jacobi, Surf. Sci. 77, (1978) L162; J. Massies, P. Etienne, F. Dezaly, and N. T. Linh, ibid 99, (1980) 121; W. Ranke and K. Jacobi, Prog. Surf. Sci. 10, (1981) 1.
9) R. Z. Bachrach, R. S. Bauer, P. Chiaradia, and G. V. Hansson, J. Vac. Sci. Technol. 19, (1981) 335.
10) P. K. Larsen, J. H. Neave, J. F. van der Veen, P. J. Dobson and B. A. Joyce, Phys. Rev. B27, (1983) 4966.
11) B. A. Joyce, J. H. Neave, P. J. Dobson and P. K. Larsen, Phys. Rev. B29, (1984) 814.
12) T. -C. Chiang, R. Ludeke, M. Aono, G. Landgren, F. J. Himpsel, and D. E. Eastman, Phys. Rev. B27, (1983) 4770.
13) D. J. Frankel, C. Yu, J. P. Harbison, and H. H. Farrell, J. Vac. Sci. Technol. B5, (1987) 1113.
14) H. H. Farrell, J. P. Harbison and L. D. Peterson, J. Vac. Sci. Technol. B5, (1987) 1482
15) M. G. Knibb and P. A. Maksym, Surf. Sci. 195, (1988) 475.
16) P. K. Larsen and D. J. Chadi, Phys. Rev. B37, (1988) 8282.
17) H. H. Farrell and C. J. Palmstrom, J. Vac. Sci. Technol. B8, (1990) 903.
18) L. Däeritz and R. Hey, Surf. Sci. 236, (1990) 15.
19) H. Yamaguchi and Y. Horikoshi, Phys. Rev. B44, (1991) 5897.
20) C. Deparis and J. Massies, J. Cryst. Growth, 108, (1991) 157.
21) J. M. McCoy, U. Korte, P. A. Maksysm and G. Meyer-Ehmsen, Phys. Rev. B48, (1993) 4721
22) H. Nöenberg and N. Koguchi, Surf. Sci. 296, (1993) 199.
23) S. P. Svensson, P. O. Nilsson and T. G. Anderson, Phys. Rev. B31, (1985) 5272.
24) R. Duszak, C. J. Palmstrom, L. T. Florez, Y. -N. Yang and J. H. Weaver, J. Vac. Sci. Technol. B10, (1992) 1891.
25) P. K. Larsen, J. H. Neave and B. A. Joyce, J. Phys. C14, (1981) 167.
26) P. K. Larsen, J. F. van der Veen, A. Mazur, J. Pollmann, J. H. Neave and B. A. Joyce, Phys. Rev. B26, (1982) 3222.
27) M. Sauvage-Simkin, R. Pinchaux, J. Massies, P. Calverie, N. Jedrecy, J. Bonnet and I. K. Robinson, Phys. Rev. Lett. 62, (1989) 563.
28) S. A. Chambers, Surf. Sci. 261, (1992) 48.
29) I. Kamiya, D. E. Aspnes, H. Tanaka, L. T. Florez, J. P. Harbison and R. Bhat, Phys. Rev. Lett. 68, (1992) 627; I. Kamiya, D. E. Aspnes, L. T. Florez and J. P. Harbison, Phys. Rev. B46, (1992) 15894.
30) K. Kanisawa, J. Osaka, S. Hirono and N. Inoue, J. Cryst. Growth, 115, (1991) 348.
31) J. Falta, R. M. Tromp, M. Copel, G. D. Pettit and P. D. Kirchner, Phys. Rev. Lett. 69, (1992) 3068; Comments and Reply, Phys. Rev. Lett. 70, (1993) 3171-3.
32) M. D. Pashley, K. W. Haberern, W. Friday, J. M. Woodall and P. D. Kirchner, Phys. Rev. Lett. 60, (1988) 2176.
33) D. K. Biegelsen, R. D. Bringans, J. E. Northrup and L. -E. Swartz, Phys. Rev. B41, (1990) 5701; D. K. Biegelsen, R. D. Bringans and L. E. Swartz, SPIE, 1186, (1990) 136.
34) M. D. Pashley and K. W. Haberern, Phys. Rev. Lett. 67, (1991) 2697; M. D. Pashley, K. W. Haberern, R. M. Feenstra and P. D. Kirchner, Phys. Rev. B48, (1993) 4612.
35) E. J. Heller, Z. Y. Zhang and M. G. Lagally, Phys. Rev. Lett. 71, (1993) 743; E. J. Heller and M. G. Lagally, Appl. Phys. Lett. 60, (1992) 2675.
36) M. Wassermeier, V. Bressler-Hill, R. Maboudian, K. Pond, X. S. Wang, W. H. Weinberg and P. M. Petroff, Surf. Sci. Lett. 278, (1992) L147; V. Bressler-Hill, M. Wassermeier, K. Pond, R. Maboudian, G. A. D. Briggs, P. M. Petroff and W. H. Weinberg, J. Vac. Sci. Technol. B10, (1992) 1881.
37) M. C. Gallagher, R. H. Prince and R. F. Willis, Surf. Sci. 275, (1992) 31.
38) H. Xu, T. Hashizume, and T. Sakurai, Jpn. J. Appl. Phys. 32, (1993) 1511.
39) S. Miwa, Y. Haga, E. Morita, S. Arakawa, T. Hashizume, and T. Sakurai, Jpn. J. Appl. Phys. 32, (1993) 1508
40) H. Yamaguchi and Y. Horikoshi, Phys. Rev. Lett. 70, (1993) 1299.
41) J. M. Zhou, Q.-K. Xue, H. Chaya, T. Hashizume and T. Sakurai, Appl. Phys. Lett. 64, (1994) 583.
42) Q.-K. Xue, J. M. Zhou, T. Hashizume and T. Sakurai, J. Appl. Phys. 75, (1994) 5021.
43) T. Hashizume, Q.-K. Xue, J. M. Zhou, A. Ichimiya and T. Sakurai, Phys. Rev. Lett. 73, (1994) 2208, Phys. Rev. B51, (1995) 4200.
44) H. Yamaguchi and Y. Horikoshi, Phys. Rev. B51, (1995) 9836.
45) Y. Hirota and T. Fukuda, Appl. Phys. Lett. 66, (1995) 2837.
46) I. Karpov, B. G. Venkateswaran, W. Gladfelter, A. Franciosi and L. Sorba J. Vac. Sci. Technol. 13 (1995) 2041.
47) M. Wassemeier, J. Behrend, L. Daweritz, and K. H. Ploog, Phys. Rev. B52, (1995) R2269.
48) A. R. Avery, D. M. Holmes, J. L. Sudijono, T. S. Jones, and B. A. Joyce, Surf. Sci. 323, (1995) 91.
49) L. D. Broekman, R. C. G. Leckey, J. D. Riley, A. Stampfl, B. F. Usher, and B. A. Sexton, Phys. Rev. B51, (1995) 17795.
50) A. R. Avery, C. M. Goringe, D. M. Holmes, J. L. Sudijono, and T. S. Jones, Phys. Rev. Lett. 76, (1996) 3344.
51) J. Behrend, M. Wassermeier, L. Daweritz, and K. H. Ploog, Surf. Sci. 342, (1996) 63.
52) Q.-K. Xue, T. Hashizume, T. Sakata, Y. Hasegawa, A. Ichimiya, T. Ohno, and T. Sakurai, Thin Solid Films 281-282, (1996) 556.
53) D. J. Chadi, J. Vac. Sci. Technol. A5, (1987) 834.
54) G. -X. Qian, R. M. Martin and D. J. Chadi, Phys. Rev. B38, (1988) 7649.
55) T. Ohno, Phys. Rev. Lett. 70, (1993) 631; ibid, 73, (1994) 460; Sci. Rep. RITU following this article.

56) J. E. Northrup and S. Froyen, Phys. Rev. Lett. 71, (1993) 2276.
57) J. E. Northrup and S. Froyen, Phys. Rev. B50, (1994) 2015.
58) W. G. Schmidt, and F. Bechstedt, Phys. Rev. B54, (1996) 16742.
59) M. D. Pashley, Phys. Rev. B40, (1989) 10481.
60) W. A. Harrison, J. Vac. Sci. Technol. 16, (1979) 1492.
61) S. L. Skala. J. S. Hubacek, J. R. Tucker, J. W. Lyding, S. T. Chou, and K. Y. Cheng, Phys. Rev. B48, (1993) 9138.
62) D. E. Aspnes, Y. C. Chang, A. A. Studna, L. T. Florez, H. H. Farrell, and J. P. Harbison, Phys. Rev. Lett. , 64, (1990) 192,
63) M. D. Pashley, Phys. Rev. Lett. 70, 3171(1993); M. Wassermier et al. ibid, 70, (1993) 3172; J. Falta et al. ibid, 70, (1993) 3173.
64) J. R. Creighton, Surface Sci. 234, (1990) 287.
65) A. Ichimiya, Jpn. J. Appl. Phys. 22, (1983) 176; Jpn. J. Appl. Phys. 24, (1985) 1365; Surf. Sci. 235, (1990) 75.
66) Q.-K. Xue, T. Hashizume, J. M. Zhou, T. Sakata, T. Sakurai, and T. Ohno, Phys. Rev. Lett. 74, (1995) 3177.
67) M. D. Pashley and K. W. Haberern, Phys. Rev. Lett. 67, (1991) 2697; M. D. Pashley, K. W. Haberern, R. M. Feenstra and P. D. Kirchner, Phys. Rev. B48, (1993) 4612.
68) Y. Horikoshi, M. Kawashima and H. Yamaguchi, Jpn. J. Appl. Phys. 25, (1986) L868.
69) Q.-K. Xue, T. Hashizume, Y. Hasegawa, and T. Sakurai, J. Cryst. Growth, in press.
70) R. M. Feenstra, J. A. Stroscio, J. Tersoff, and A. P. Fein, Phys. Rev. Lett. 25, (1987) 1192.
71) P. K. Lasen, P. J. Dobson, J. H. Neave, B. A. Joyce, B. Böger and J. Zhang, Surf. Sci. 169, (1986) 176.
72) A. Ichimiya et al. , to be published.
73) G. M. Lagally, in "Methods of experimental Physics," (Academic Press, 1985) 237; Henzler, Surf. Sci. 11/12, (1982) 450.
74) I. M. Vitomirov, A. D. Raisanen, A. C. Finnefrock, R. E. Viturro, L. J. Brillson, P. D. Kirchner, G. D. Pettit, and J. M. Woodall, J. Vac. Sci. Technol. B10, (1992) 1898.
75) T. Hashizume, K. Motai, X. D. Wang, H. Shinohara, Y. Saito, Y. Murayama, K. Ohno, Y. Kawazoe, Y. Nishina, H. W. Pickering, Y. Kuk and T. Sakurai, Phys. Rev. Lett. 71, (1993) 2959.
76) T. Sakurai, T. Hashizume, I. Kamiya, Y. Hasegawa, N. Sano, H. W. Pickering, and A. Sakai, Prog. Surf. Sci. 33, (1990) 3; T. Hashizume, I. Sumita, Y. Murata, S. Hypdo, and T. Sakurai, J. Vac. Sci. Technol. A9, (1991) 742.
77) M. D. Pashley and K. W. Haberen, Ultramicroscopy, 42-44, (1992) 1281.
78) M. D. Pashley, K. W. Haberern, and R. M. Feenstra, J. Vac. Sci. Technol. B10, (1992) 1874.
79) T. Ohno, private communication.
80) Haihua. Qi, P. E. Gee, and R. F. Hicks, Phys. Rev. Lett. 72, (1994) 250.
81) Q.-K. Xue, T. Ogino, Y. Hasegawa, H. Shinohara and T. Sakurai, Phys. Rev. B53, (1996) 1985.
82) H. W. M. Salemink, M. B. Johnson, and O. Albrektsen, J. Vac. Sci. Technol. B12, (1994) 362
83) C. F. McConville, T. S. Jones, F. M. Leibsle, S. M. Driver, T. C. Q. Noakes, M. O. Schweitzer, and N. V. Richardson, Phys. Rev. B50, (1994) 14965.
84) J. Cerda, F. J. Palomares, and F. Soria, Phys. Rev. Lett. , 75, (1995) 665.
85) M. -H. Tsai, C. F. Liu, and C. S. Chang, Phys. Rev. B54, (1996) 7637.
86) A complete review is published in Prog. Surf. Sci. (1997).